

# Accepted Manuscript

New 4-phenylcoumarin derivatives as potent 3C protease inhibitors: Design, synthesis, anti-HAV effect and molecular modeling

Asmaa F. Kassem, Rasha Z. Batran, Eman M.H. Abbas, Samia A. Elseginy, Mohamed N. Shaheen, El-Mahdy M. El-Mahdy



PII: S0223-5234(19)30162-X

DOI: <https://doi.org/10.1016/j.ejmech.2019.02.048>

Reference: EJMECH 11140

To appear in: *European Journal of Medicinal Chemistry*

Received Date: 26 November 2018

Revised Date: 31 January 2019

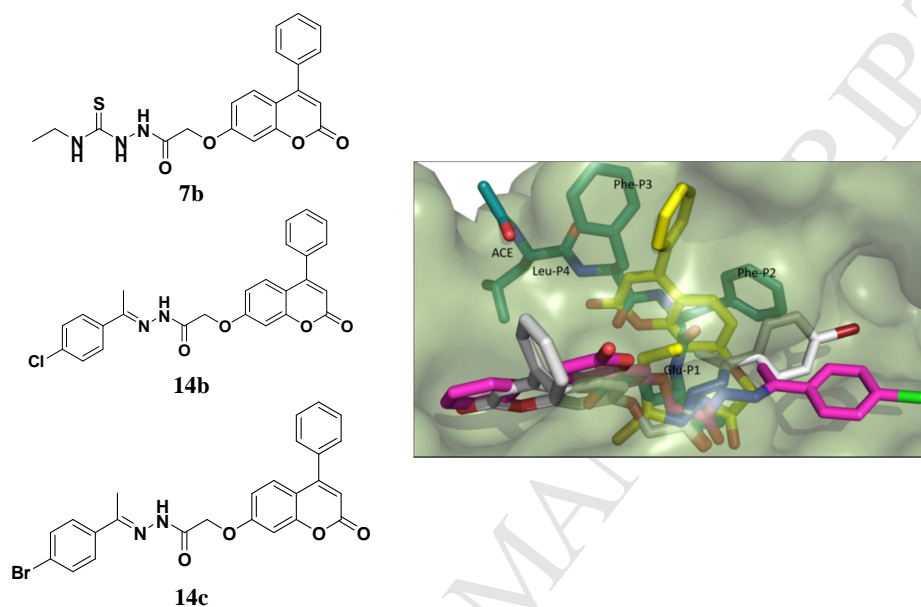
Accepted Date: 14 February 2019

Please cite this article as: A.F. Kassem, R.Z. Batran, E.M.H. Abbas, S.A. Elseginy, M.N. Shaheen, E.-M.M. El-Mahdy, New 4-phenylcoumarin derivatives as potent 3C protease inhibitors: Design, synthesis, anti-HAV effect and molecular modeling, *European Journal of Medicinal Chemistry* (2019), doi: <https://doi.org/10.1016/j.ejmech.2019.02.048>.

This is a PDF file of an unedited manuscript that has been accepted for publication. As a service to our customers we are providing this early version of the manuscript. The manuscript will undergo copyediting, typesetting, and review of the resulting proof before it is published in its final form. Please note that during the production process errors may be discovered which could affect the content, and all legal disclaimers that apply to the journal pertain.

## Graphical Abstract

## New 4-phenylcoumarin derivatives as potent 3C protease inhibitors: Design, synthesis, anti-HAV effect and molecular modeling



	7b	14b	14c
HAV(IC <sub>50</sub> , TI)	3.1 μg/mL, 83 (virucidal)	10.7 μg/mL, 91 (virustatic) (viral replication)	8.5 μg/mL, 88 (virustatic) (viral adsorption)
HAV 3C <sup>pro</sup> (Ki)	1.903 μM	0.104 μM	0.217 μM
HRV 3C <sup>pro</sup> (IC <sub>50</sub> )	16.1 μM	4.13 μM	6.3 μM

## New 4-phenylcoumarin derivatives as potent 3C protease inhibitors: Design, synthesis, anti-HAV effect and molecular modeling

Asmaa F. Kassem,<sup>a</sup> Rasha Z. Batran,<sup>b\*</sup> Eman M.H. Abbas,<sup>a</sup> Samia A. Elseginy,<sup>c</sup> Mohamed N. Shaheen,<sup>d</sup> El-Mahdy M. El-Mahdy<sup>d</sup>

<sup>a</sup> *Chemistry of Natural and Microbial Products Department, Pharmaceutical and Drug Industries Research Division, National Research Centre, 33 El Bohouth St., Dokki, Giza, p.o.box 12622, Egypt*

<sup>b</sup> *Chemistry of Natural Compounds Department, Pharmaceutical and Drug Industries Research Division, National Research Centre, 33 El Bohouth St., Dokki, Giza, p.o. box 12622, Egypt*

<sup>c</sup> *Green Chemistry Department, Chemical Industries Research Division, National Research Centre, 33 El Bohouth St., Dokki, Giza, p.o. box 12622, Egypt*

<sup>d</sup> *Environmental Virology laboratory, Water pollution Research Department, Environmental Research Division, National Research Centre, 33 El Bohouth St., Dokki, Giza, p.o. box 12622, Egypt*

\*Corresponding author: rasha\_batran@yahoo.com

### Abstract

A new series of 4-phenylcoumarin derivatives was synthesized starting from (2-oxo-4-phenyl-2H-chromen-7-yloxy) acetic acid hydrazide **3**. Evaluation of the target compounds for their antiviral activity against hepatitis A virus revealed that the ethylthiosemicarbazide derivative **7b** was the most potent virucidal agent ( $IC_{50}=3.1\mu\text{g/mL}$ ,  $TI = 83$ ). The Schiff's bases **14c** and **14b** demonstrated the highest virustatic effects against viral adsorption and replication, respectively (**14c**;  $IC_{50}=8.5\mu\text{g/mL}$ ,  $TI = 88$  and **14b**;  $IC_{50}=10.7\mu\text{g/mL}$ ,  $TI = 91$ ). Furthermore, compounds **7b**, **14b** and **14c** were tested against HAV 3C protease and showed significant inhibition effects ( $K_i= 1.903, 0.104$  and  $0.217\mu\text{M}$ , respectively). The remarkable inhibitory effect expressed by the three target compounds against HAV 3C protease prompted us to expand our research on HRV 3C protease, a structurally related enzyme of the same family, and interestingly, the three target compounds displayed significant inhibitory effect against HRV 3C protease ( $IC_{50}= 16.10, 4.13$  and  $6.30\mu\text{M}$ ,

respectively). Moreover, the active compounds **7b**, **14b** and **14c** were docked within the pocket site of HAV 3C protease (PDB code: 2HAL) illustrating a strong H-profile with the key amino acids Gly170 and Cys172 similar to the co-crystallized ligand. Furthermore, 3D-pharmacophore and quantitative structure activity relationship (QSAR) models were generated to explore the structural requirements for the observed antiviral activity.

Keywords: 4-phenylcoumarins; heterocyclic; anti-HAV; 3C protease; docking; QSAR; 3D pharmacophore.

## 1. Introduction

Picornaviruses, family *Picornaviridae*, are positive-strand non enveloped RNA viruses comprising important human pathogens such as human rhinovirus (HRV), poliovirus (PV), encephalomyocarditis virus and hepatitis A virus (HAV)[1]. Regulated proteolysis is an essential feature in the processing of the picornaviral polyprotein (250 kDa) that is crucial for replication process [2]. As such, picornaviruses evolve highly specific proteases, 3C proteases (3C<sup>pro</sup>) sharing similar spatial structures. These proteases are responsible for processing the polyprotein precursor and also cleaving certain cellular factors needed for transcription and translation processes as well as nucleocytoplasmic trafficking in order to modulate cell physiology for viral replication thus 3C<sup>pro</sup> play a principle role in the viral life cycle which might expose viral proteases as selective targets for antiviral therapy [3].

Hepatitis A is a highly contagious liver disease caused by hepatitis A virus (HAV). It is a self-limited acute disease usually transmitted *via* fecal-oral route. Infection with HAV causes fever, weakness, malaise, myalgias, arthralgias, anorexia, vomiting, and nausea [4-6]. Fulminant hepatitis A is a rare but devastating complication of HAV infection that leads to acute liver failure (ALF) which is a potential lethal disease [7]. Elderly patients and those with chronic liver disease are at a higher risk for fulminant hepatitis A [8]. Although millions of infection cases are yearly reported, with much higher incidence in developing countries, there are no commercially available anti-HAV drugs till date. Similar to other picornaviruses, HAV genome encodes a main processing protease, assigned HAV 3C (HAV 3C<sup>pro</sup>) which is a nonstructural cysteine protein responsible for the cleavage process within the viral polyprotein which is critical for the replication process.

The chromene scaffold represents a functional core structure in various biologically active anti-picornaviral agents and 3C protease inhibitors. Flavonoids, 2-

phenyl-4*H*-chromen-4-ones, as luteoloside [9], quercetin [10], rutin and fisetin [11] have been reported for their antiviral effectiveness against EV71 which was mediated by the inhibition of 3C protease enzymatic activity and hence blocking viral replication. Recently, synthetic chromene analogues have been considered as promising biodynamic pharmacophores for designing and development of anti-picornaviral therapeutic agents [12-16].

Coumarins (2*H*-chromen-2-ones) are recognized as a privileged bioactive scaffold for designing new agents with high affinity and specificity to various molecular targets, [17-20] especially as antiviral agents [21-25]. 4-Phenylcoumarins (neoflavones), bioisosteres of flavonoids, gained great attention in the past few decades as lead target structures for the discovery of new antiviral agents [26,27]. Although the antiviral effectiveness of various coumarin compounds has already been published, the anti-HAV potential of coumarin derivatives remains largely unexplored.

In view of these observations, momentous attention has been paid to make use of the structural isosterism between the 4-phenylcoumarin scaffold and the flavonid structural core to develop new modified 4-phenylcoumarin-based drug candidates as new 3C protease inhibitors.

We report herein the synthesis of new 4-phenylcoumarin derivatives hybridized with acyclic thiosemicarbazide and imine functionalities as well as various five membered azaheterocyclic rings, reported for their anti-HAV effect, such as pyrrol, pyrazole, oxadiazole, thiadiazole and triazole moieties and the study of their antiviral activities against hepatitis A [28-34]. The most active anti-HAV derivatives were further assessed for their inhibitory potential towards HAV 3C<sup>pro</sup>.

Molecular docking was performed for the most active anti-HAV candidates within the pocket site of HAV 3C protease (PDB code: 2HAL). Moreover, QSAR and pharmacophore methodology were used to identify the structural features required for the antiviral properties of these new series. In addition, drug likeness properties of the new series were investigated in order to identify the oral bioavailability of the new 4-phenylcoumarin derivatives.

## 2. Results and discussion

### 2.1. Chemistry

The 4-phenyl-7-oxycoumarin derivatives **1-4**, **5a-c**, **6**, **7a,b**, **8a,b**, **9a,b**, **10-12**, **13a-c** and **14a-c** were efficiently synthesized according to the procedures outlined in **schemes 1-4**.

A facile synthesis of the key intermediate hydrazide **3** [35] involves the reaction of the ester compound **2** [35] and hydrazine hydrate in ethyl alcohol at room temperature (**Scheme 1**).

The 5-thioxo-1,3,4-oxadiazole derivative **4** [35] was prepared by refluxing the hydrazide **3** with carbon disulfide in pyridine. Compound **4** was further S-alkylated with dimethylaminoethyl chloride hydrochloride, diethylaminoethyl chloride hydrochloride and/or 2-morpholinoethyl chloride hydrochloride, in refluxing dry acetone in the presence of anhydrous potassium carbonate, to afford the target dimethylaminoethylthio-1,3,4-oxadiazole **5a**, diethylaminoethylthio-1,3,4-oxadiazole **5b** and morpholinoethylthio-1,3,4-oxadiazoles **5c**, respectively. On the other hand, hydrazinolysis of the 5-thioxo-1,3,4-oxadiazole derivative **4** with hydrazine hydrate in refluxing ethyl alcohol afforded the 4-amino-5-mercapto-1,2,4-triazole derivative **6** (**Scheme 2**).

The thiosemicarbazide derivatives **7a,b** [17] were obtained through the condensation of the hydrazide **3** with methylisothiocyanate and / or ethylisothiocyanate, respectively. Heterocyclization of the thiosemicarbazides **7a,b** with H<sub>2</sub>SO<sub>4</sub> gave the corresponding aminothiadiazoles **8a,b**, respectively. While, condensing thiosemicarbazide derivatives **7a,b** with 2N potassium hydroxide solution afforded the corresponding N-(methyl/ ethyl)-5-thioxo-1,2,4-triazole derivatives **9a,b**. The 7-((5-(2-morpholinoethylthio)-4-ethyl-4*H*-1,2,4-triazol-3-yl) methoxy)-4-phenyl-2*H*-chromen-2-one **10** was prepared *via* refluxing 4-ethyl-5-thioxo-1,2,4-triazole **9b** with 2-morpholinoethyl chloride hydrochloride, in dry acetone in the presence of anhydrous potassium carbonate (**Scheme3**).

Cyclocondensation of the hydrazide **3** with acetylacetone afforded the corresponding 3,5-dimethylpyrazole **11**. The target 2-(4-phenylcoumarin-7-yloxy)-N-(1,3-dioxoisindolin-2-yl) acetamide **12** [35] was obtained by the condensation of the hydrazide **3** with phthalic anhydride in acetic acid, while refluxing the hydrazide **3** with isatin derivatives, namely; isatin, 6-chloroisatin and / or 6-bromoisatin, yielded the corresponding oxoindolin-3ylidene acetohydrazides **13a-c**. Moreover, the Schiff's

bases **14 a-c** were obtained by the condensation of the hydrazide compound **3** with acetophenone derivatives, namely; acetophenone, 4-chloroacetophenone and/ or 4-bromoacetophenone (Scheme 4). The structures of the new compounds were characterized by means of IR, <sup>1</sup>HNMR, <sup>13</sup>CNMR and EI-MS.

## 2.2. Biology

### 2.2.1. Antiviral Screening

In this work we reported the anti-HAV activity of the synthesized target compounds. The cytotoxicity test was conducted to determine the safe doses which could be used in the antiviral assays. Safe concentrations were used to determine the antiviral effect of the compounds through three different assays to understand the mechanism by which these compounds can inhibit the virus infection.

In virucidal experiment, the tested compounds showed therapeutic index ranging from 0.2 to 83, where five compounds **1**, **4**, **7b**, **9a** and **13c** displayed therapeutic index higher than 50 (TI = 70.8, 78, 83, 57, 73, respectively) (**Table 1**). The target compounds may exert virucidal activity through the interaction with the viral capsid changing its configuration and causing inability of the virus to bind to the cell receptor. The bioactive compounds may also interact with the capsid proteins resulting in the prevention of the virus entry into host cells. In the pre-treatment assay, the compounds showed therapeutic index ranging from 0.2 to 88 where **5b**, **7a**, **12** and **14c** compounds exhibited therapeutic index higher than 50 (TI = 77, 80, 72, and 88, respectively) (**Table 1**). These findings indicate that the target compounds inhibited virus infection through the effect on virus adsorption to the cell surface. These compounds may interfere with virus binding by blocking the cellular receptors and hence lead to the anti-HAV effect. During the post-treatment assay, the compounds showed therapeutic index ranging from 0.1 to 91 where **4**, **10**, **13c** and **14b** showed strong antiviral activity with TI ≥ 50 (TI = 50, 70, 52 and 91, respectively) (**Table 1**). In this experiment, the virus inhibition may be due to the interaction of the target compounds with one or more viral enzyme needed to complete the replication cycle or due to the interference with one step or more in the viral life cycle.

### 2.2.2. Inhibition of HAV 3C protease

In this study, the most active compounds against hepatitis A **7b**, **14b** and **14 c** were further screened to identify potent inhibitors of the picornaviral HAV 3C<sup>pro</sup>. The three compounds showed promising inhibitory effect against HAV 3C<sup>pro</sup> with Ki values of 1.903, 0.104 and 0.217 μM, respectively (**Table 2**).

Both the 4-chlorophenyl Schiff's base **14b** and the 4-bromophenyl congener **14c** showed significant inhibitory constants at low micromolar concentrations ( $K_i=0.104$  and  $0.217 \mu\text{M}$ , respectively) indicating strong binding to HAV 3C<sup>pro</sup>.

### 2.2.3. Inhibition of HRV 3C protease

The significant inhibitory effect of compounds **7b**, **14b** and **14c** against HAV 3C<sup>pro</sup> encouraged us to expand our research area to discover novel 3C protease inhibitors, we have tested the inhibitory effect of the three target compounds **7b**, **14b** and **14c** against another structurally related picornaviral 3C protease, HRV 3C<sup>pro</sup> as a screening procedure and guidance for future investigation on a panel of the same family proteases as an important step in anti-picornaviral drug discovery. The three compounds showed promising inhibition effects with  $IC_{50}$  values of 16.10, 4.13 and  $6.30 \mu\text{M}$ , respectively, almost with similar  $IC_{50}$  values to that displayed against HAV 3C<sup>pro</sup> (**Table 2**). The aforementioned results indicate that the target compounds are non selective 3C protease inhibitors as such could be important lead compounds for future discovery of broad spectrum 3C protease inhibitors.

### 2.3. Structure activity relationship

The 7-hydroxy-4-phenylcoumarin **1** showed high virucidal effect with  $IC_{50}=4.8 \mu\text{g/ml}$  and  $TI=70.8$ . The activity was diminished for the ester **2** and the hydrazide derivative **3** ( $IC_{50}=1285.7, 3925 \mu\text{g/ml}$ ,  $TI=0.7, 0.2$ ). The post treatment assay revealed that compound **2** can moderately affect viral replication ( $IC_{50}=25.7 \mu\text{g/ml}$ ,  $TI=35$ ).

The thioxo-1,3,4-oxadiazole **4** elicited significant virucidal potency ( $IC_{50}=4.7 \mu\text{g/ml}$ ,  $TI=78$ ) and remarkable effect on viral replication ( $IC_{50}=7.34 \mu\text{g/ml}$ ,  $TI=50$ ). Furthermore, S-alkylation of the thioxo-1,3,4-oxadiazolyl derivative **4** with dimethylaminoethyl moiety **5a** decreases both the virucidal effect ( $IC_{50}=44.8 \mu\text{g/ml}$ ,  $TI=20$ ) and the viral replication potency ( $IC_{50}=35.8 \mu\text{g/ml}$ ,  $TI=25$ ). Although the diethylaminoethyl derivative **5b** was devoid of any virucidal effect ( $IC_{50}=81.6 \mu\text{g/ml}$ ,  $TI=3$ ), it exhibited potent effect on viral adsorption ( $IC_{50}=3.18 \mu\text{g/ml}$ ,  $TI=77$ ) and moderate effect on viral replication ( $IC_{50}=0.75 \mu\text{g/ml}$ ,  $TI=32$ ). The morpholinoethyl derivative **5c** showed decreased anti-HAV effect for both virucidal activity and effect on viral adsorption ( $IC_{50}=9.9 \mu\text{g/ml}$ ,  $TI=25$ ), and diminished effect on viral replication ( $IC_{50}=622.5 \mu\text{g/ml}$ ,  $TI=0.4$ ).

The thiosemicarbazides **7a,b** demonstrated potent anti-HAV activities. The ethylthiosemicarbazide derivative **7b** was the most potent virucidal agent

( $IC_{50}$ =3.1 $\mu$ g/ml,  $TI$ = 83). It demonstrated higher antiviral effect than the standard drug acyclovir ( $IC_{50}$ = 35.6  $\mu$ g/ml,  $TI$ = 80). While, the methyl congener **7a** showed significant effect on viral adsorption ( $IC_{50}$ = 11.88  $\mu$ g/ml,  $TI$ = 80). On the other hand, cyclization of the thiosemicarbazides into aminothiadiazoles **8a,b** completely diminished the antiviral activity.

Within the cyclized triazole series both N-methyl/ and N-ethyl thioxotriazoles **9a,b** showed the highest virucidal effects ( $IC_{50}$ = 11.3, 12.9  $\mu$ g/ml,  $TI$ = 57,46) while, the 7-((5-(2-morpholinoethylthio)-4-ethyl-4H-1,2,4-triazol-3-yl) methoxy)- 4-phenylcoumarin **10** was significantly the most potent antiviral agent affecting viral replication ( $IC_{50}$ = 13.4 $\mu$ g/ml,  $TI$ = 70). The N-amino-mercaptotriazole **6** was devoid of any anti-HAV effect.

The 3,5-dimethylpyrazole derivative **11** displayed decreased virucidal effect with  $IC_{50}$ = 37.6 $\mu$ g/ml and  $TI$ = 20. It also displayed weak effect on viral replication ( $IC_{50}$ = 44.3 $\mu$ g/ml,  $TI$ = 17).

The target bromoindolyl-4-phenylcoumarin **13c** exhibited remarkable improved anti-HAV properties. It demonstrated significant virucidal effect ( $IC_{50}$ = 13 $\mu$ g/ml,  $TI$ = 73) and remarkable effects on both viral replication ( $IC_{50}$ = 18.3  $\mu$ g/ml,  $TI$ = 52) and adsorption ( $IC_{50}$ = 21.6  $\mu$ g/ml,  $TI$ = 44). The isoindole derivative **12** elicited high antiviral potency through its effect on viral adsorption ( $IC_{50}$ =13  $\mu$ g/ml,  $TI$ = 72). On the other hand the unsubstituted indolyl derivative **13a** and the chloroindolyl-4-phenylcoumarin **13b** completely lacked any anti-viral effects against HAV.

Additionally, the 4-chlorophenyl Schiff's base **14b** was the most potent anti-HAV agent affecting viral replication among all the synthesized compounds ( $IC_{50}$ = 10.7 $\mu$ g/ml,  $TI$ = 91), with comparable activity to the standard drug Acyclovir ( $IC_{50}$ = 30.6  $\mu$ g/ml,  $TI$ = 93). It had moderate virucidal effect ( $IC_{50}$ = 30.5 $\mu$ g/ml,  $TI$ = 32) along with decreased effect on viral adsorption ( $IC_{50}$ = 44.4 $\mu$ g/ml,  $TI$ = 22). Furthermore, the 4-bromophenyl congener **14c** proved to be the most potent compound affecting viral adsorption ( $IC_{50}$ = 8.5  $\mu$ g/ml,  $TI$ = 88) with higher activity than the standard drug ( $IC_{50}$ = 35.5  $\mu$ g/ml,  $TI$ = 85), while it had weak effect on viral replication ( $IC_{50}$ =62.5 $\mu$ g/ml,  $TI$ = 12). The antiviral activity was completely diminished for the unsubstituted phenyl Schiff's base derivative **14a**.

## 2.4. Molecular modeling study

### 2.4.1. Molecular docking

The crystal structure of HAV 3C protease (PDB code: 2CXV) [36] revealed that the enzyme binds to the substrate at four or five residues (P4 to P1; Leu, Arg, Thr and Gln) [37]. The mode of action proceeds through a nucleophilic attack of Cys172 thiolate on the substrate carbonyl oxygen with base assistance from His44. Also, hydrogen bond between His191 and carbonyl oxygen in the side chain of glutamine (P1) was shown in this crystal structure [37]. In 2006 Jiang *et al* [38], solved the crystal structure of HAV 3C with tetrapeptidyl-based methyl ketone inhibitor at high resolution (PDB:2HAL) [36], the tetrapeptide portion of these inhibitors are analogous to the residues at P4 to P1 in the natural substrate position. Tetrapeptidyl inhibitor (N-acetyl-Leucyl-phenylalanyl-phenylalanyl-glutamate) formed two covalent bonds between P1-Glutamine and Cys172, and H-bond with Gly170 [38] (**Fig.1**). P3-phenylalanine formed two H-bonds with Val144 and Gly194 (**Fig.1**), P4-Leucin contributed by two H-bonds with Val144 and Gly194 (**Fig. 1, Table 3**).

In our modeling study we docked the three active compounds **7b**, **14b** and **14c** within the pocket site of HAV 3C protease (PDB code: 2HAL), MOE [39] software was used to build the compounds and minimize the energy while docking studies were carried out with Autodock4 [40].

The docking results showed that compound **7b** illustrated interactions with the key residues Gly170 and Cys 172 and formed four H-bonds in a similar manner to the tetrapeptidyl inhibitor where, O atom of C=O of compound **7b** formed two hydrogen bonds with SH-Cys172 and additional two H-bonds one with NH of Cys172 and one with NH –Gly170 (**Fig.2A**), the four H-bonds formed net-like structure that stabilized the compound within the binding pocket. The C=O of coumarin moiety formed H-bond with NH of Gly194 which is another key amino acid at a distance of 2.9Å (**Fig.2B**). Unexpectedly the sulfur atom of the linker side chain received H from NH-Hist191, this amino acid showed an important interaction with C=O of glutamine (P1), in the previous crystal structure (PDB:code 2CXV). The inhibitory activity of compound **7b** was attributed to these H-bonds and the hydrophobic interaction with Pro169 and Ala193 (**Fig2, Table 3**).

Compounds **14b** and **14c** are analogues, the difference was only in the *p*-phenyl substituent and this explains the similarity between the two compounds in the interactions and fitting within the binding pocket of HAV 3C protease. Oxygen atom of C=O moiety of compounds **14b** and **14c** showed the same H-profiles; O atom formed two H- bonds with the SH-Cys172, the most important amino acid for the

activity. Also, O atom formed two H bonds with NH-Cys172 and NH-Gly172. The 4-phenyl coumarin moiety showed hydrophobic interactions with Leu168, pro169, Ala193 and the hydrophobic part of Gly194 and Gly195 (**Figs. 3 and 4, Table 3**).

#### 2.4.2. Binding Modes of compounds **7b**, **14b** and **14c**

To further predict the possible binding mode for each compound within the pocket site of HAV 3C protease, the binding free energy ( $\Delta G_{\text{Bind}}$ ) and binding affinity  $pK_d$  were determined (**Table 4**).

The binding mode of the three compounds was represented in **Figure 5**. Compound **7b** ( $K_i = 1.903 \mu\text{M}$ ) showed good binding mode as 4-phenylcoumarin moiety occupied the same position as P2-phenylalanine and P3-phenylalanine, and the side chain filled the same space similar to P1-glutamine. It had the highest  $\Delta G_{\text{Bind}}$  and binding affinity  $pK_d$  ( $\Delta G_{\text{Bind}} = -9.15 \text{ kcal/mol}$ ,  $pK_d = 6.78$ ). Compounds **14b** and **14c** ( $K_i = 0.104$  and  $0.217 \mu\text{M}$ , respectively) exhibited the same binding mode as P1-glutamine of the tetrapeptidyl inhibitor displaying comparable  $\Delta G_{\text{Bind}}$  and binding affinity  $pK_d$  ( $\Delta G = -7.44$  and  $-7.47 \text{ kcal/mol}$ ,  $pK_d = 5.51$  and  $5.53$ ).

It could be seen that the three inhibitors **7b**, **14b** and **14c** illustrated a strong H-profile with the key amino acids Gly170 and Cys172 in a similar manner to the tetrapeptidyl inhibitor; the co-crystallized ligand which explains the inhibitory activity of these compounds and displayed relative favorable binding free energy and binding affinity. These results were in agreement with the biological findings and it proved the importance of Cys172 residue for enzyme activity. The potential interactions of compounds **7b**, **14b** and **14c** within the active site of HAV 3C protease provide significant rationale as to the mechanism by which these compounds suppress HAV 3C protease activity. Nevertheless, experimental analysis is required to validate the predicted binding mode of the three compounds.

#### 2.4.3. QSAR studies

QSAR studies were carried out for the coumarin derivatives that showed a virucidal inhibitory activity. The data set was divided randomly as training set (18 compounds) and a test set (5 compounds) with their measured  $pIC_{50}$  ( $-\log IC_{50}$ ). The molecular operating environment (MOE) software [41] was employed for the calculation of the physicochemical descriptors of the molecules. 2D and 3D QSAR descriptors were calculated; 2D descriptors include physical properties, subdivided subsurface areas, adjacency and distance and partial charge descriptors. 3D

descriptors include potential Energy, MOPAC, surface Area, volume and shape descriptors and conformation dependent charge descriptors.

Partial least square (PLS) method was used to perform the study. The models underwent validation study by internal methods *via* leave one-out cross-validation (LOO),  $r^2$  (squared correlation coefficient),  $r^2$  prediction (predictive squared correlation coefficient), Z-outlier score and residuals between the experimental and predicted activity [42].

In this study volume surface vsurf\_Wp (3D descriptor), density (3D descriptor) and opr\_brigid (2D descriptor), contribute for the best predicted activity and the highest  $r^2$  (0.8). vsurf\_Wp descriptor describes the polar volume of the molecules [43], in general, Wp1-4 account for dispersion forces and polarizability while Wp5-8 account for polar and hydrogen bond donor/ acceptor regions [43]. Additionally, opr\_brigid descriptor describes the number of rigid bonds.

QSAR models were represented graphically by scattering plots of the experimental versus the predicted bioactivity (**Fig.6**). Partial least square (PLS) method was used to build the QSAR models,  $r^2=0.891$ , root mean square error (RMSE) = 0.200, cross validation  $r^2=0.671$  and cross validation RMSE= 0.351.

In conclusion, the virucidal activity of the synthesized compounds is correlated negatively with vsurf\_Wp4, vsurf\_Wp6, and opr\_rigid., but is correlated positively with density. The virucidal activity decreased with the increase in the H-bond donor/or acceptor groups on molecules' surface and with the increase in the polarizability of the molecules. Also, the virucidal activity decreased with the increase in the number of rigid bonds of the molecules. On the other hand, the antiviral activity increased with the rise in density. It is interesting to note that although compound **7b** had higher vsurf\_Wp4 and vsurf-Wp6, it possessed the best virucidal effect which may be due to its lower number of rigid bonds. These findings are relevant for the design of novel antiviral agents and these structure-based approaches may lead to improved virucidal activity for the next generation.

QSAR models were validated internally applying leave-1-out cross-validation where  $r^2$  (squared correlation coefficient value) is 0.891, cross validation  $r^2=0.671$  and RMSE = 0.200 which is a small error value. Validation was also employed by measuring the residuals between the experimental activity and the predicted activity (**Table 5**). It is noticeable that the residuals between the predicted antiviral activity

and the experimental one are very close, indicating the reliability and effectiveness of the established QSAR mode. Also, Z-outlier values of the training set were less than 2

#### 2.4.4. Pharmacophore modeling

In this study, pharmacophore generation was performed using MOE software, the pharmacophore query editor protocol was used to generate the pharmacophore from a set of ligands with known antiviral activity values. The pharmacophore features which were used are hydrogen bond acceptor (HBA), hydrogen bond donor (HBD), hydrophobic interactions (HYD) and ring aromatic (RA). Different pharmacophore models (hypothesis) were generated *via* flexible aligning of different conformations of the best five compounds with the best antiviral activity. The top pharmacophore was generated including seven features; two HBA, one HBD, three RA, and one HYD (**Fig.7**). The constraint distances and angles between pharmacophore features are represented in **table 6**.

Compound **7b** and **4** are represented with the best generated pharmacophore model (**Fig.8**). Seven features of the pharmacophore were considered, where compound **7b** (**Fig.8A**) fitted with six features out of seven, where carbonyl group and oxygen atom fitted with two features (HBA), coumarin moiety and phenyl group fitted with three (RA) and NH fitted with (HBD). While compound **4** fitted with five features out of seven, where carbonyl group and oxygen atom fitted with two features (HBA), coumarin moiety and phenyl group fitted with three (RA).

The results of pharmacophore supported the results of QSAR analysis as the pharmacophore features include only one HBD and 2HDA. QSAR results suggested that the antiviral activity decreased with the increase in the number of H-bond donors or acceptors.

#### 2.4.5. Drug likeness properties

The twenty three synthesized compounds were assessed against Lipinski's rule [44]. Briefly, the rule is based on the observation that most orally administered drugs have a molecular weight (MW) of 500 or less, five or fewer hydrogen bond donor sites, ten or fewer hydrogen bond acceptor sites and Log P should not be greater than 5. In addition, the polar surface area (PSA), was calculated, since it is another key property that has been linked to the drug bioavailability. Thus, passively absorbed molecules with a PSA >140 Å are thought to have low oral bioavailability [45]. The results showed that our compounds fulfilled Lipinski's rule expect compound **13c** which violated the rule in the MW and compounds **5c**, **9a,b** and **14a-c** that broke the

rule in the logP by a little difference, whilst the active compounds **1,4,5c,7b** and **9a** fulfilled Lipinski's rule (**Table 7**). Although the active compound **13c** broke the rule, it is still expected to be orally bioactive, because the rule states that an orally active drug has no more than one violation of rule of five or Lipinski's rule. In addition, the compounds also fulfilled the topological surface area. The most active compound **7b** fulfilled the Lipinski's rule and PSA which indicates that it has a good oral bioavailability.

### 3. Conclusion

A new series of 4-phenylcoumarin derivatives was synthesized and the target compounds were evaluated for their antiviral effect against hepatitis A virus through studying their virucidal activity, effect on viral adsorption and effect on viral replication in the host cell. The ethylthiosemicarbazide derivative **7b** displayed the highest virucidal effect among the tested target compounds ( $IC_{50}=3.1\mu\text{g/ml}$ ,  $TI = 83$ ). The 4-bromophenyl Schiff's base **14c** was the most potent compound affecting viral adsorption ( $IC_{50}=8.5\mu\text{g/ml}$ ,  $TI = 88$ ) while the 4-chlorophenyl congener **14b** showed the most significant potential on viral replication ( $IC_{50}=10.7\mu\text{g/ml}$ ,  $TI = 91$ ). Furthermore, compounds **7b**, **14c** and **14b** were tested against HAV 3C protease revealing significant inhibition effects ( $IC_{50}= 17.78, 7.19$  and  $5.94\mu\text{M}$ , respectively).

The three compounds showed promising inhibition effect against the structurally related protease HRV 3C<sup>pro</sup> with  $IC_{50}$  values of 16.1, 4.13 and  $6.3\mu\text{M}$ , respectively. On the other hand, molecular docking study was performed between the three inhibitors **7b**, **14b** and **14c** and HAV 3C protease, which illustrated a strong H-profile with the key amino acids Gly170 and Cys172 in a similar manner to the co-crystallized ligand tetrapeptidyl inhibitor which explains the inhibitory activity of these compounds. The combined analysis of QSAR and 3D pharmacophore revealed significant information on the structural requirement for promising antiviral activity. Several QSAR models were generated and the best one showed  $r^2=0.891$ , root mean square error (RMSE) = 0.200. The best four descriptors of the selected model were vsurf\_Wp4, vsurf-Wp6, density and opr\_brigid. The generated 3D pharmacophore showed 7 features; two HBA, one HBD, three RA, and one HYD. The molecular modeling results may have a significant role in proposing further optimization directions for designing more potent second generation antiviral agents. Docking and pharmacophore modeling study proved the importance of coumarin moiety in the binding mode of the promising compounds **7b**, **14a** and **14c** within the active site of

HAV3C protease and hence their promising enzymatic inhibitory activity. Based on QSAR results, optimization of 4-phenylcoumarin derivatives could be achieved by designing new derivatives with more hydrophobic characters by introducing less polar substituents and also, linking 4-phenylcoumarin scaffold to flexible substituent groups. The bioactive candidates **7b**, **14a** and **14c** are predicted to have good oral bioavailability according to Lipinski's rule and PSA.

## 4. Experimental

### 4.1. Chemistry

All melting points were uncorrected and measured using Electrothermal IA 9000 apparatus. Infrared spectra were measured by Nexus 670 FT-IR FT-Raman spectrometer using KBr discs at National Research Center, Cairo, Egypt. <sup>1</sup>HNMR spectra were determined using Varian mercury 300 MHz spectrometer at Micro-Analytical Laboratory, Central Services Laboratory, Faculty of Science, Cairo University, Egypt and Bruker 400 MHz spectrometer at Faculty of Pharmacy, Ain Shams University, Egypt, using TMS as the internal standard. <sup>13</sup>CNMR spectra were determined using Varian mercury 300 MHz spectrometer and 400 MHz spectrometer. The mass spectra were recorded on GCMS-QP 1000EX Shimadzu Gas Chromatography MS Spectrometer. <sup>13</sup>CNMR, Mass Spectra and the elemental analyses were performed at Micro-Analytical Laboratory, Central Services Laboratory, Faculty of Science, Cairo University, Egypt. The reactions were followed by TLC (silica gel, aluminum sheets 60 F254, Merck) using chloroform-methanol (9.5:0.5 v/v) as eluent and sprayed with iodine-potassium iodide reagent. The purity of the newly synthesized compounds was assessed by TLC and elemental analysis and was found to be higher than 95%. Compounds **1** [46], **2** [47], **3** [35], **4** [35], **6** [35] and **12** [35] were previously prepared.

#### **General procedure for the preparation of 7-((5-[(2-(dimethylamino)ethylthio), 2-(diethylamino)ethylthio) and / or (2-morpholinoethylthio)]-1,3,4-oxadiazol-2-yl)methoxy)-4-phenyl-2H-chromen-2-one (5a-c)**

A mixture of **4** (3.52g, 0.01 mol), dimethylaminoethyl chloride hydrochloride, diethylaminoethyl chloride hydrochloride, and/or 4-(2-chloroethyl) morpholine hydrochloride (0.03mol) and anhydrous potassium carbonate (4.2 g, 0.03 mol) in dry acetone (100 mL) was refluxed while stirring for 10–15 hours. The mixture was filtered while hot, the filtrate was concentrated, and water was added to precipitate the desired target compounds which were recrystallized from acetone/water.

**7-((5-(2-(Dimethylamino)ethylthio)-1,3,4-oxadiazol-2-yl)methoxy)-4-phenyl-2H-chromen-2-one (5a)**

Off white powder, yield 76 %, mp 122-4°C. Anal. Calcd.: C, 62.40; H, 5.00; N, 9.92; S, 7.57. Found: C, 62.55; H, 5.18; N, 10.12; S, 7.67. IR (cm<sup>-1</sup>, KBr): 3067 (CH aromatic stretching), 2944, 2932 (CH aliphatic stretching), 1726 (C=O,  $\alpha$ -pyrone). <sup>1</sup>HNMR (300MHz, DMSO-*d*<sub>6</sub>,  $\delta$ , ppm): 2.17 (6H, s, 2CH<sub>3</sub>N), 2.58-2.62 (2H, t, CH<sub>2</sub>N), 3.38-3.41 (2H, t, CH<sub>2</sub>S), 5.55 (2H, s, OCH<sub>2</sub>), 6.29 (1H, s, H-3 coumarin), 7.27-7.59 (8H, m, Ar-H). <sup>13</sup>CNMR (75MHz, DMSO-*d*<sub>6</sub>,  $\delta$ , ppm): 30.8, 44.7, 57.2, 59.9, 102.4, 112.1, 112.8, 128.0, 128.4, 128.9, 129.7, 134.9, 154.9, 155.2, 159.7, 160.2, 162.9, 165.6. EI-MS (m/z) for C<sub>22</sub>H<sub>21</sub>N<sub>3</sub>O<sub>4</sub>S (423.13): 423 [M]<sup>+</sup> (0.53%), 72 (100.00%).

**7-((5-(2-(Diethylamino)ethylthio)-1,3,4-oxadiazol-2-yl)methoxy)-4-phenyl-2H-chromen-2-one (5b)**

White powder, yield 70%, mp 78-80°C. Anal. Calcd.: C, 63.84; H, 5.58; N, 9.31; S, 7.10. Found: C, 63.64; H, 5.45; N, 9.19; S, 6.98. IR (cm<sup>-1</sup>, KBr): 3061 (CH aromatic stretching), 2956, 2936 (CH aliphatic stretching), 1727 (C=O,  $\alpha$ -pyrone). <sup>1</sup>HNMR (300MHz, DMSO-*d*<sub>6</sub>,  $\delta$ , ppm): 0.90-0.95 (6H, t, 2CH<sub>3</sub>CH<sub>2</sub>N), 2.45-2.49 (4H, q, 2CH<sub>3</sub>CH<sub>2</sub>N), 2.73-2.77 (2H, t, CH<sub>2</sub>N), 3.34-3.38 (2H, t, CH<sub>2</sub>S), 5.55 (2H, s, OCH<sub>2</sub>), 6.29 (1H, s, H-3 coumarin), 7.02-7.59 (8H, m, Ar-H). <sup>13</sup>CNMR (75MHz, DMSO-*d*<sub>6</sub>,  $\delta$ , ppm): 14.2, 30.9, 44.7, 57.2, 59.9, 102.4, 112.1, 112.8, 127.9, 128.4, 128.8, 129.6, 134.9, 154.9, 155.5, 159.7, 160.2, 162.9, 165.6. EI-MS (m/z) for C<sub>24</sub>H<sub>25</sub>N<sub>3</sub>O<sub>4</sub>S (451.16): 451 [M]<sup>+</sup> (0.14%), 86 (100.00%).

**7-((5-(2-Morpholinoethylthio)-1,3,4-oxadiazol-2-yl)methoxy)-4-phenyl-2H-chromen-2-one (5c)**

White powder, yield 70%, mp 120-2 °C. Anal. Calcd.: C, 61.92; H, 4.98; N, 9.03; S, 6.89. Found: C, 62.24; H, 5.10; N, 9.19; S, 6.95. IR (cm<sup>-1</sup>, KBr): 3060 (CH aromatic stretching), 2943, 2932 (CH aliphatic stretching), 1729 (C=O,  $\alpha$ -pyrone). <sup>1</sup>HNMR (300MHz, CDCl<sub>3</sub>,  $\delta$ , ppm): 2.49-2.53 (4H, t, 2 CH<sub>2</sub>N morpholine), 2.76- 2.81 (2H, t, CH<sub>2</sub>N), 3.43-3.48 (2H, t, CH<sub>2</sub>S), 3.67-3.71 (4H, t, 2 CH<sub>2</sub>O morpholine), 5.30 (2H, s, OCH<sub>2</sub>), 6.27 (1H, s, H-3 coumarin), 6.89-7.54 (8H, m, Ar-H). <sup>13</sup>CNMR (75MHz, DMSO-*d*<sub>6</sub>,  $\delta$ , ppm): 30.5, 48.7, 54.2, 60.6, 61.1, 102.4, 111.7, 112.5, 112.9, 127.8, 128.3, 128.7, 129.5, 134.8, 151.7, 154.9, 155.1, 159.7, 160.5, 166.1. EI-MS (m/z) for C<sub>24</sub>H<sub>23</sub>N<sub>3</sub>O<sub>5</sub>S (465.14): 465 [M]<sup>+</sup> (0.21%), 100 (100%).

**General Procedure for the preparation of 1-(2-(2-oxo-4-phenyl-2H-chromen-7-yloxy)acetyl)-4-methyl and / or ethylthiosemicarbazide 7a,b.**

To a solution of the hydrazide **3** (3.1g, 0.01 mol) in hot absolute ethanol, methylisothiocyanate and/or ethylisothiocyanate (0.01mol) was added. The mixture was refluxed for 5-7 hours and the separated solid was filtered, washed with ethanol and recrystallized from acetic acid.

**1-(2-(2-Oxo-4-phenyl-2H-chromen-7-yloxy)acetyl)-4-methylthiosemicarbazide 7a [17].**

White powder, yield 85%, mp 217–9°C. Anal. Calcd.: C, 59.52; H, 4.47; N, 10.96; S, 8.36. Found: C, 59.64; H, 4.63; N, 11.19; S, 8.48. IR (cm<sup>-1</sup>, KBr): 3399, 3376, 3310 (3NH), 1702 (C=O,  $\alpha$ -pyrone), 1670 (C=O), 1242 (C=S). <sup>1</sup>HNMR (300MHz, DMSO-*d*<sub>6</sub>,  $\delta$ , ppm): 2.88-2.89 (3H, d, CH<sub>3</sub>), 4.74 (2H, s, OCH<sub>2</sub>), 6.26 (1H, s, H-3 coumarin), 6.81–7.57 (8H, m, Ar–H), 7.83-7.85 (1H, q, NHCH<sub>3</sub>, D<sub>2</sub>O exchangeable), 10.18 (1H, s, NH, D<sub>2</sub>O exchangeable), 13.91(1H, s, NH, D<sub>2</sub>O exchangeable). EI-MS (m/z) for C<sub>19</sub>H<sub>17</sub>N<sub>3</sub>O<sub>4</sub>S (383.09): 383 [M]<sup>+</sup> (13%), 163 (100%).

**1-(2-(2-Oxo-4-phenyl-2H-chromen-7-yloxy)acetyl)-4-ethylthiosemicarbazide 7b [17].**

White powder, yield 80%, mp 219–21°C. Anal. Calcd.: C, 60.44; H, 4.82; N, 10.57; S, 8.07. Found: C, 60.34; H, 4.71; N, 10.49; S, 7.91. IR (cm<sup>-1</sup>, KBr): 3385, 3376, 3325, (3NH), 1708 (C=O,  $\alpha$ -pyrone), 1675 (C=O), 1242 (C=S). <sup>1</sup>HNMR (300MHz, DMSO-*d*<sub>6</sub>,  $\delta$ , ppm): 1.05-1.09 (3H, t, CH<sub>3</sub>), 3.47-3.49 (2H, m, CH<sub>2</sub>), 4.73 (2H, s, OCH<sub>2</sub>), 6.26 (1H, s, H-3 coumarin), 6.99–7.57 (8H, m, Ar–H), 7.99-8.02 (1H, t, NHCH<sub>2</sub>, D<sub>2</sub>O exchangeable), 9.19 (1H, s, NH, D<sub>2</sub>O exchangeable), 10.08 (1H, s, NH, D<sub>2</sub>O exchangeable). EI-MS (m/z) for C<sub>20</sub>H<sub>19</sub>N<sub>3</sub>O<sub>4</sub>S (397.11): 397 [M]<sup>+</sup> (3%), 161 (100%).

**Preparation of 7-((5-((methyl and /or ethyl) amino)-1,3,4-thiadiazol-2-yl)methoxy)-4-phenyl-2H-chromen-2-one 8a,b.**

An appropriate thiosemicarbazide **7a** and/or **7b** (0.001 mol) was dissolved in concentrated sulphuric acid (1.6 mL), cooled and allowed to stand for 30 minutes at 0°C while stirring. The reaction mixture was added gradually to crushed ice. The separated solid was filtered off, washed with water till acid free, dried and recrystallized from acetic acid.

**7-((5-(Methylamino)-1,3,4-thiadiazol-2-yl)methoxy)-4-phenyl-2H-chromen-2-one 8a.**

White powder, yield 75%, mp 180-2°C. Anal. Calcd.: C, 62.45; H, 4.14; N, 11.50; S, 8.78. Found: C, 62.35; H, 4.01; N, 11.39; S, 8.67. IR (cm<sup>-1</sup>, KBr): 3303 (NH), 1676 (C=O,  $\alpha$ -pyrone). <sup>1</sup>HNMR (400MHz, DMSO-*d*<sub>6</sub>,  $\delta$ , ppm): 2.88-2.89 (3H, d, CH<sub>3</sub>), 5.45 (2H, s, OCH<sub>2</sub>), 6.27 (1H, s, H-3 coumarin), 6.99–7.58 (8H, m, Ar–H), 7.82-7.86 (1H, q, NH, D<sub>2</sub>O exchangeable). <sup>13</sup>CNMR (75MHz, DMSO-*d*<sub>6</sub>,  $\delta$ , ppm): 30.9, 64.8, 102.4, 111.8, 112.5, 112.9, 128.0, 128.4, 128.9, 129.7, 134.9, 152.2, 154.9, 155.3, 159.8, 160.6, 169.9. EI-MS (m/z) for C<sub>19</sub>H<sub>15</sub>N<sub>3</sub>O<sub>3</sub>S (365.08): 365 [M]<sup>+</sup> (2.83%), 128 (100.00%).

**7-((5-(Ethylamino)-1,3,4-thiadiazol-2-yl)methoxy)-4-phenyl-2H-chromen-2-one 8b.**

White powder, yield 85%, mp 188-90°C. Anal. Calcd.: C, 63.31; H, 4.52; N, 11.07; S, 8.45. Found: C, 63.20; H, 4.42; N, 10.97; S, 8.38. IR (cm<sup>-1</sup>, KBr): 3305 (NH), 1670 (C=O,  $\alpha$ -pyrone). <sup>1</sup>HNMR (300MHz, DMSO-*d*<sub>6</sub>,  $\delta$ , ppm): 1.14-1.19 (3H, t, CH<sub>3</sub>), 3.26-3.29 (2H, m, CH<sub>2</sub>), 5.44 (2H, s, OCH<sub>2</sub>), 6.26 (1H, s, H-3 coumarin), 6.99–7.56 (8H, m, Ar–H), 7.82-7.85 (1H, t, NH, D<sub>2</sub>O exchangeable). <sup>13</sup>CNMR (75MHz, DMSO-*d*<sub>6</sub>,  $\delta$ , ppm): 14.2, 37.9, 64.8, 102.5, 111.8, 112.5, 112.9, 127.9, 128.4, 128.8, 129.6, 134.9, 152.2, 154.9, 155.3, 159.8, 160.6, 169.9. EI-MS (m/z) for C<sub>20</sub>H<sub>17</sub>N<sub>3</sub>O<sub>3</sub>S (379.1): 380 [M+1]<sup>+</sup> (22.23%), 379 [M]<sup>+</sup> (7.3%), 189 (100%).

**Preparation 7-((4-methyl and / or ethyl)-5-thioxo-1,2,4-triazol-3-yl)methoxy)-4-phenyl-2H-chromen-2-one 9a,b.**

A solution of **7a** and / or **7b** (0.01 mol) in 2N KOH (30 ml) was refluxed for 4-6 hours. The mixture was cooled, acidified with dil. HCl, filtered, washed with water and recrystallized from ethanol.

**7-((4-Methyl-5-thioxo-1,2,4-triazol-3-yl)methoxy)-4-phenyl-2H-chromen-2-one 9a.**

White powder, yield 75%, mp 240–2°C. Anal. Calcd.: C, 62.45; H, 4.14; N, 11.50; S, 8.78. Found: C, 62.57; H, 4.25; N, 11.67; S, 8.89. IR (cm<sup>-1</sup>, KBr): 3350 (NH), 1685 (C=O,  $\alpha$ -pyrone). <sup>1</sup>HNMR (300MHz, DMSO-*d*<sub>6</sub>,  $\delta$ , ppm): 3.51 (3H, s, CH<sub>3</sub>), 5.39 (2H, s, OCH<sub>2</sub>), 6.28 (1H, s, H-3 coumarin), 6.81–7.56 (8H, m, Ar–H), 13.80 (1H, s, NH, D<sub>2</sub>O exchangeable). <sup>13</sup>CNMR (75MHz, DMSO-*d*<sub>6</sub>,  $\delta$ , ppm): 30.5, 61.1, 102.4, 111.7, 112.5, 112.8, 127.8, 128.3, 128.7, 129.5, 134.8, 151.7, 154.9, 155.1, 159.7, 160.5, 168.2. EI-MS (m/z) for C<sub>19</sub>H<sub>15</sub>N<sub>3</sub>O<sub>3</sub>S (365.08): 365 [M]<sup>+</sup> (43.96%), 238 (100.00%).

**7-((4-Ethyl-5-thioxo-1,2,4-triazol-3-yl)methoxy)-4-phenyl-2H-chromen-2-one 9b.**

White powder, yield 85%, mp 194-6 °C. Anal. Calcd.: C, 63.31; H, 4.52; N, 11.07; S, 8.45. Found: C, 63.21; H, 4.41; N, 10.98; S, 8.39. IR (cm<sup>-1</sup>, KBr): 3351 (NH), 1687 (C=O,  $\alpha$ -pyrone). <sup>1</sup>HNMR (400MHz, DMSO-*d*<sub>6</sub>,  $\delta$ , ppm): 1.25-1.29 (3H, t, CH<sub>3</sub>), 4.02-4.07 (2H, q, CH<sub>2</sub>), 5.41 (2H, s, OCH<sub>2</sub>), 6.29 (1H, s, H-3 coumarin), 7.03–7.57 (8H, m, Ar–H), 13.92 (1H, s, NH, D<sub>2</sub>O exchangeable). <sup>13</sup>CNMR (100MHz, DMSO-*d*<sub>6</sub>,  $\delta$ , ppm): 13.8, 29.8, 60.8, 102.9, 112.4, 113.2, 113.4, 128.5, 128.9, 129.3, 130.2, 135.3, 147.8, 155.5, 155.7, 160.3, 160.6, 167.7. EI-MS (m/z) for C<sub>20</sub>H<sub>17</sub>N<sub>3</sub>O<sub>3</sub>S (379.1): 379 [M]<sup>+</sup> (23.14%), 211(100.00%).

**Preparation of 7-((5-(2-morpholinoethylthio)-4-ethyl-4H-1,2,4-triazol-3-yl)methoxy)-4-phenyl-2H-chromen-2-one 10.**

A mixture of **9b** (0.38g, 0.001 mol), 4-(2-chloroethyl) morpholine hydrochloride (0.56g, 0.003 mol) and anhydrous potassium carbonate in dry acetone (100 ml) was refluxed while stirring for 10-15 hours. The mixture was filtered while hot, the filtrate was concentrated and water was added to precipitate the desired target compounds which were recrystallized from acetone/water.

White powder, yield 78%, mp 150-2°C. Anal. Calcd.: C, 63.40; H, 5.73; N, 11.37; S, 6.51. Found: C, 63.28; H, 5.61; N, 11.26; S, 6.42. IR (cm<sup>-1</sup>, KBr): 2949- 2931 (CH aliphatic stretching), 1698 (C=O,  $\alpha$ -pyrone). <sup>1</sup>HNMR (300MHz, DMSO-*d*<sub>6</sub>,  $\delta$ , ppm): 1.25-1.30 (3H, t, CH<sub>3</sub>CH<sub>2</sub>), 2.33-2.36 (4H, t, 2CH<sub>2</sub>N morpholine), 2.59-2.64 (2H, t, CH<sub>2</sub>N), 3.31-3.36 (2H, t, CH<sub>2</sub>S), 3.47-3.49 (4H, t, 2CH<sub>2</sub>O morpholine), 4.02-4.05 (2H, q, CH<sub>2</sub>CH<sub>3</sub>), 5.46 (2H, s, OCH<sub>2</sub>), 6.27 (1H, s, H-3 coumarin), 7.02–7.58 (8H, m, Ar–H). <sup>13</sup>CNMR (100MHz, DMSO-*d*<sub>6</sub>,  $\delta$ , ppm): 15.6, 30.5, 53.3, 53.4, 57.9, 60.8, 66.5, 102.8, 112.3, 112.9, 113.4, 126.7, 128.4, 128.5, 128.9, 129.3, 130.2, 135.3, 151.0, 151.6, 155.5, 155.7, 160.3, 160.9. EI-MS (m/z) for C<sub>26</sub>H<sub>28</sub>N<sub>4</sub>O<sub>4</sub>S (492.18): 492 [M]<sup>+</sup> (0.39%), 113 (100%).

**Preparation of 7-(2-(3,5-dimethyl-1H-pyrazol-1-yl)-2-oxoethoxy)-4-phenyl-2H-chromen-2-one 11.**

A mixture of the hydrazide **3** (0.31g, 0.001 mol) and acetylacetone (0.001 mol, 0.1 mL) in 20 mL absolute ethanol was refluxed for about 12 hours while stirring. The formed precipitate after cooling was filtered, dried and recrystallized from ethyl alcohol.

White powder, yield 79%, mp 164-166 °C. Anal. Calcd.: C, 70.58; H, 4.85; N, 7.48. Found: C, 70.69; H, 4.91; N, 7.53. IR (cm<sup>-1</sup>, KBr): 1707 (C=O,  $\alpha$ -pyrone), 1678 (C=O amide). <sup>1</sup>HNMR (300MHz, DMSO-*d*<sub>6</sub>,  $\delta$ , ppm): 2.22 (3H, s, CH<sub>3</sub>-pyrazole),

2.47 (3H, s, CH<sub>3</sub>-pyrazole), 5.63 (2H, s, OCH<sub>2</sub>), 6.23 (1H, s, CH-pyrazole), 6.25 (1H, s, H-3 coumarin), 6.98- 7.57 (8H, m, Ar-H). <sup>13</sup>CNMR (75MHz, DMSO-*d*<sub>6</sub>, δ, ppm): 13.5, 13.5, 66.5, 102.3, 111.3, 111.6, 112.4, 112.6, 127.8, 128.4, 128.8, 129.6, 134.98, 143.7, 152.5, 155.0, 155.3, 159.8, 161.7, 167.4. EI-MS (m/z) for C<sub>22</sub>H<sub>18</sub>N<sub>2</sub>O<sub>4</sub> (374.13): 374 [M]<sup>+</sup> (28.2 %), 109 (100%).

**Preparation of 2-(2-oxo-4-phenyl-2*H*-chromen-7-yloxy)-N'-(5-(un)substituted-2-oxoindolin-3-ylidene) acetohydrazide 13a-c**

A mixture of hydrazide **3** (3.1g, 0.01 mol) and the appropriate isatin compounds, namely, isatin, 5-chloroisatin and/or 5-bromoisatin (0.01 mol) in absolute ethanol (30 mL) containing glacial acetic acid (1mL) was refluxed while stirring for 8-10 hours. The reaction mixture was cooled and the formed solid was collected by filtration and recrystallized from acetic acid to give the target compounds.

**2-(2-Oxo-4-phenyl-2*H*-chromen-7-yloxy)-N'-(2-oxoindolin-3-ylidene) acetohydrazide 13a**

Yellow powder, yield 80%, mp 273-5°C. Anal. Calcd.: C, 68.33; H, 3.90; N, 9.56. Found: C, 68.28; H, 3.81; N, 9.48. IR (cm<sup>-1</sup>, KBr): 3367, 3311 (2NH), 1707 (C=O, α-pyrone), 1689 (C=O, isatin), 1616 (C=O, hydrazide). <sup>1</sup>HNMR (300MHz, DMSO-*d*<sub>6</sub>, δ, ppm): 5.01 (2H, s, OCH<sub>2</sub>), 6.26 (1H, s, H-3 coumarin), 6.93-7.59 (12H, m, Ar-H), 11.25 (1H, s, NH, D<sub>2</sub>O exchangeable), 13.81 (1H, s, NH, D<sub>2</sub>O exchangeable). <sup>13</sup>CNMR (100MHz, DMSO-*d*<sub>6</sub>, δ, ppm): 67.7, 102.7, 111.7, 112.4, 113.2, 120.1, 121.5, 123.1, 128.5, 128.9, 129.2, 129.3, 130.2, 132.4, 135.4, 143.1, 155.4, 155.7, 160.3, 162.9. EI-MS (m/z) for C<sub>25</sub>H<sub>17</sub>N<sub>3</sub>O<sub>5</sub> (439.12): 439 [M]<sup>+</sup> (6.2 %), 175 (100%).

**2-(2-Oxo-4-phenyl-2*H*-chromen-7-yloxy)-N'-(5-chloro-2-oxoindolin-3-ylidene)acetohydrazide 13b**

Orange crystals, yield 85%, mp 118-20°C. Anal. Calcd.: C, 63.37; H, 3.40; N, 8.87. Found: C, 63.29; H, 3.33; N, 8.78. IR (cm<sup>-1</sup>, KBr): 3371, 3325(2NH), 1711 (C=O, α-pyrone), 1689 (C=O, isatin), 1615 (C=O, hydrazide). <sup>1</sup>HNMR (300MHz, DMSO-*d*<sub>6</sub>, δ, ppm): 5.03 (2H, s, OCH<sub>2</sub>), 6.24 (1H, s, H-3 coumarin), 6.88-7.56 (11H, m, Ar-H), 11.23 (1H, s, NH, D<sub>2</sub>O exchangeable), 13.66 (1H, s, NH, D<sub>2</sub>O exchangeable). <sup>13</sup>CNMR (75MHz, DMSO-*d*<sub>6</sub>, δ, ppm): 66.5, 102.5, 111.9, 112.6, 113.0, 120.9, 120.9, 127.6, 128.2, 128.3, 128.7, 129.5, 129.8, 131.3, 134.9, 137.5, 143.7, 155.1, 155.3, 159.9, 160.6, 168.5. EI-MS (m/z) for C<sub>25</sub>H<sub>16</sub>ClN<sub>3</sub>O<sub>5</sub> (473.08): 475/473 [M+2]<sup>+</sup>/ [M]<sup>+</sup> (8.97/23.72%), 209 (100.00%).

**2-(2-Oxo-4-phenyl-2H-chromen-7-yloxy)-N'-(5-bromo-2-oxoindolin-3-ylidene)acetohydrazide 13c**

Orange crystals, yield 82%, mp 120-2°C. Anal. Calcd.: C, 57.93; H, 3.11; N, 8.11. Found: C, 58.05; H, 3.22; N, 8.20. IR (cm<sup>-1</sup>, KBr): 3373, 3329 (2NH), 1710 (C=O,  $\alpha$ -pyrone), 1687 (C=O, isatin), 1618 (C=O, hydrazide). <sup>1</sup>HNMR (300MHz, DMSO-*d*<sub>6</sub>,  $\delta$ , ppm): 5.02 (2H, s, OCH<sub>2</sub>), 6.26 (1H, s, H-3 coumarin), 6.90–7.57 (11H, m, Ar-H), 11.25 (1H, s, NH, D<sub>2</sub>O exchangeable), 13.78 (1H, s, NH, D<sub>2</sub>O exchangeable). <sup>13</sup>CNMR (75MHz, DMSO-*d*<sub>6</sub>,  $\delta$ , ppm): 66.40, 101.9, 111.7, 112.5, 112.9, 120.4, 120.5, 123.0, 128.2, 128.3, 128.7, 129.5, 129.8, 131.3, 134.8, 137.5, 144.8, 154.9, 155.2, 159.7, 160.4, 166.1. EI-MS (m/z) for C<sub>25</sub>H<sub>16</sub>BrN<sub>3</sub>O<sub>5</sub> (517.03): 519/517 [M+2]<sup>+</sup>/ [M]<sup>+</sup> (1.29/ 1.24%), 57 (100.00%).

**Preparation of 2-(2-Oxo-4-phenyl-2H-chromen-7-yloxy)-N'-(1-(4-(un)substituted phenyl) ethylidene) acetohydrazide 14a-c**

A mixture of hydrazide compound **3** (3.1g, 0.01 mol) and acetophenone compounds, namely; acetophenone, 4-chloroacetophenone and/or 4-bromoacetophenone (0.01 mol) in absolute ethanol in the presence of glacial acetic acid (2mL), was refluxed for 6-8 hours, the formed precipitate was filtered off, dried and recrystallized from acetic acid.

**2-(2-Oxo-4-phenyl-2H-chromen-7-yloxy)-N'-(1-phenylethylidene)acetohydrazide 14a**

White powder, yield 90%, mp 218-20 °C. Anal. Calcd.: C, 72.80; H, 4.89; N, 6.79. Found: C, 72.75; H, 4.82; N, 6.68. IR (cm<sup>-1</sup>, KBr): 3180 (NH), 1717 (C=O,  $\alpha$ -pyrone), 1682 (C=O). <sup>1</sup>HNMR (300MHz, DMSO-*d*<sub>6</sub>,  $\delta$ , ppm): 2.33 (3H, s, CH<sub>3</sub>), 5.33 (2H, s, OCH<sub>2</sub>), 6.22 (1H, s, H-3 coumarin), 6.99-7.87 (13H, m, Ar-H), 10.82 (1H, s, NH, D<sub>2</sub>O exchangeable). <sup>13</sup>CNMR (75MHz, DMSO-*d*<sub>6</sub>,  $\delta$ , ppm): 13.3, 65.8, 101.9, 111.7, 112.5, 112.9, 127.6, 128.2, 128.3, 128.8, 129.5, 129.8, 131.3, 134.8, 137.8, 148.7, 154.8, 155.0, 159.7, 160.4, 168.6. EI-MS (m/z) for C<sub>25</sub>H<sub>20</sub>N<sub>2</sub>O<sub>4</sub> (412.14): 414 [M+2]<sup>+</sup> (21.54%), 412 [M]<sup>+</sup> (12.4%), 219 (100%).

**2-(2-Oxo-4-phenyl-2H-chromen-7-yloxy)-N'-(1-(4-chlorophenyl)ethylidene) acetohydrazide 14b**

White powder, yield 85 %, mp 258-9°C. Anal. Calcd.: C, 67.19; H, 4.29; N, 6.27. Found: C, 67.25; H, 4.33; N, 6.36. IR (cm<sup>-1</sup>, KBr): 3188 (NH), 1710 (C=O,  $\alpha$ -pyrone), 1686 (C=O). <sup>1</sup>HNMR (300MHz, DMSO-*d*<sub>6</sub>,  $\delta$ , ppm): 2.27 (3H, s, CH<sub>3</sub>), 5.35 (2H, s, OCH<sub>2</sub>), 6.24 (1H, s, H-3 coumarin), 6.99–7.87 (12H, m, Ar-H), 10.95 (1H, s, NH,

D<sub>2</sub>O exchangeable). <sup>13</sup>CNMR (100MHz, DMSO-*d*<sub>6</sub>, δ, ppm): 13.9, 66.2, 102.5, 111.9, 112.4, 113.2, 128.2, 128.5, 128.8, 128.9, 129.3, 130.1, 134.4, 135.5, 137.2, 147.9, 155.6, 155.7, 160.4, 162.0, 169.7. EI-MS (m/z) for C<sub>25</sub>H<sub>19</sub>ClN<sub>2</sub>O<sub>4</sub> (446.1): 448/446 [M+2]<sup>+</sup>/ [M]<sup>+</sup> (26.03/66.69%), 209 (100.00%).

**2-(2-Oxo-4-phenyl-2H-chromen-7-yloxy)-N'-(1-(4-bromophenyl)ethylidene) acetohydrazide 14c**

White powder, yield 95%, mp 265-7°C. Anal. Calcd.: C, 61.11; H, 3.90; N, 5.70. Found: C, 61.21; H, 3.98; N, 5.81. IR (cm<sup>-1</sup>, KBr): 3200 (NH), 1719 (C=O, α-pyrone), 1688 (C=O). <sup>1</sup>HNMR (300MHz, DMSO-*d*<sub>6</sub>, δ, ppm): 2.34 (3H, s, CH<sub>3</sub>), 5.38 (2H, s, OCH<sub>2</sub>), 6.23 (1H, s, H-3 coumarin), 6.97–7.88 (12H, m, Ar-H), 10.57 (1H, s, NH, D<sub>2</sub>O exchangeable). <sup>13</sup>CNMR (75MHz, DMSO-*d*<sub>6</sub>, δ, ppm): 13.9, 66.4, 101.9, 111.9, 112.6, 113.0, 127.6, 128.2, 128.3, 128.8, 129.5, 129.8, 131.3, 134.9, 137.9, 148.7, 154.9, 155.2, 159.7, 163.1, 171.1. EI-MS (m/z) for C<sub>25</sub>H<sub>19</sub>BrN<sub>2</sub>O<sub>4</sub> (490.05): 492/490 [M+2]<sup>+</sup>/ [M]<sup>+</sup> (30.99/ 30.71%), 253 (100.00%).

## 4.2. Biology

### 4.2.1. Anti-HAV assay

#### 4.2.1.1. Cell culture and virus

A fetal rhesus monkey kidney cell line (Frhk-4), Purchased from VACSERA-Egypt, cultured in DMEM (Dulbecco's Modified Eagle Medium) enriched with 10% of FBS (fetal bovine serum), 100 units/ml, 100µg/ml streptomycin, penicillin under 5% CO<sub>2</sub> incubator. Hepatitis A virus (HAV) prepared in ten-fold dilution was inoculated onto cell lines in 96 well plate. After 72 h of inoculation, the cytopathic effect was investigated under inverted microscope and TCID<sub>50</sub>/0.1ml (50% tissue culture infectious doses/0.1 ml) was estimated according to Karber method [48], then the tittered stock distributed into small aliquots and stored at – 80°C until used.

#### 4.2.1.2. Cytotoxicity assay

The cytotoxicity of the compounds on Frhk-4 cell lines was performed by MTT [3-(4,5- dimethylthiazol-2-yl)-2,5-diphenyl tetrazolium bromide] assay, as described by Nabil *et al* [49]. In brief, the cells at concentration 5 X 10<sup>3</sup> cells / well were seeded in 96- well plates. After incubation period for 24 hours, the cell medium was discarded and the cell monolayers were incubated with various concentrations (ranging from 7.8 - 1000 µg/mL) of each compound followed by incubation period for additional 48 hours at 37 °C under 5% CO<sub>2</sub> atmosphere. The compounds were removed and 100 µL of MTT solution (5 mg/mL) was added for 4 hours at 37°C.

After removing MTT, 50  $\mu$ L dimethyl sulfoxide (DMSO) was added to cells. After 30 minutes at 37°C, the optical density was checked at 540 nm using a multiwell ELISA reader. The  $CC_{50}$  (50% cytotoxic concentration) was estimated as  $(K - B / K) \times 100$ , where K and B are the mean of three  $OD_{540}$  of untreated and treated cells with compounds, respectively.

#### **4.2.1.3. Antiviral effect of the tested compounds by MTT method**

Frhk-4cell lines were seeded in 96- well plates and after 24 hours incubation, the cell medium was removed from the wells and the antiviral experiment was conducted in three different approaches.

##### **4.2.1.3.1. Virucidal assay**

The virus ( $10^6$  log<sub>10</sub> TCID<sub>50</sub>/0.1 ml) was mixed and incubated with equal volume of various non-toxic concentrations of each compound for 1 hour at 37°C. Then 100  $\mu$ l of the previous mixture was added and incubated with cell monolayers for 1hour. After that, the mixture was removed from wells and replaced with culture medium.

##### **4.2.1.3.2. Pre-treatment assay**

The cell monolayers grown in 24-well plates were treated and incubated with various non-toxic concentrations of each compound for 24 hours at 37°C under 5% CO<sub>2</sub> atmosphere. The compound concentrations were removed and replaced with virus suspension. After 1 hour at 37°C, then viral suspension was removed and replaced with culture medium.

##### **4.2.1.3.3. Post-treatment assay**

The confluent cell monolayers were infected with virus suspension. After 1 hour, the unbound virus was removed and replaced with test medium containing various non-toxic concentrations of each compounds.

In the three experiments, positive control (virus-infected cells) and negative control wells (only cells with culture medium) were included. After incubating all plates for 72 hours under 5% CO<sub>2</sub> atmosphere at 37°C. The mean of three  $OD_{540}$  of treated cells, positive control, and negative control were read on multiwall ELISA reader then  $IC_{50}$  (the 50% inhibitory concentration) was estimated as  $[(K-V)/(C-V) \times 100]$ , where K, V and C refer to the mean three absorbance values of treated cells, positive control, and negative control, respectively. The therapeutic index (TI) for each compound was calculated by dividing of  $CC_{50} / IC_{50}$ .

#### 4.2.2. HAV 3C<sup>pro</sup> determination assay

##### 4.2.2.1. Protein expression and purification

The HAV 3C<sup>pro</sup> was produced heterologously using *Escherichia coli* BL21(DE3) pLysS containing pHAV-3CEX according to the reported procedures [50].

##### 4.2.2.2. Fluorogenic peptide assay

The steady-state proteolytic activities of HAV 3C was measured using the fluorogenic peptide substrate Dabcyl-GLRTQSDN (edans) G. The standard assay was performed using 0.1 M potassium phosphate, pH 7.5, 2 mM EDTA containing 0.1  $\mu$ M protease and 10–75  $\mu$ M peptide at 37 °C. Substrate (10  $\mu$ M) and inhibitor (0.25–10  $\mu$ M) were pre-warmed for three minutes in black 96-well microplates in a total volume of 200  $\mu$ l before the reaction was started with the addition of enzyme ( $\lambda_{\text{ex}}$ = 355 nm,  $\lambda_{\text{em}}$ = 460 nm). Initial inhibitor screening and IC<sub>50</sub> determination for HAV 3C<sup>pro</sup> were done using a 96-well plate and a Victor <sup>2</sup> fluorescence plate reader [50]. The Ki value for each inhibitor candidate was calculated using the Cheng and Prusoff equation [51].

##### 4.2.3. HRV 3C<sup>pro</sup> determination assay

Inhibition activities of compounds **7b**, **14b** and **14c** against HRV 3C<sup>pro</sup> were measured colorimetrically using ab211089 HRV 3C Protease Inhibitor Screening Kit according to the manufacturer instructions.

All materials and prepared reagents were equilibrated to room temperature prior to use. The reaction wells were set up where, the screening sample wells contain 10  $\mu$ L of the tested compounds, the enzyme control wells contain 10  $\mu$ L assay buffer and the solvent control wells contain 10  $\mu$ L solvent. The HRV 3C protease enzyme solution (50  $\mu$ L/well) was prepared by adding 2  $\mu$ L of HRV 3C– protease to 48  $\mu$ L of assay buffer, mixed well and added into each well then the plate was incubated at room temperature for 15 minutes. Additionally, 40  $\mu$ L of the substrate mixture was prepared by adding 5  $\mu$ L of HRV 3C– substrate to 35  $\mu$ L of assay buffer, added to each well and mixed well. The absorbance was measured at OD 405 nm in kinetic mode for 1 – 2 hours at 37°C.

#### 4.3. Molecular modeling

##### 4.3.1. Molecular docking

The crystal structure of HAV 3C protease in complex with tetrapeptidyl methyl ketone was retrieved from The RCSB DAT Bank (PDB:2HAL). Ligand structures were built with MOE2008 software, and the energy was minimized using the MMFF94x force field. Docking studies were carried out using autodock4 software where, the native ligand was re-docked to investigate the validity of the docking protocol, the docking site was considered using the position of the tetrapeptidyl inhibitor and grid box was set to -6.457, -6.566, 36.559 dimensions. The photos were created using Pymol software. Binding free energy ( $\Delta G_{\text{Bind}}$ ) and binding affinity  $pK_d$  were calculated *via* PlayMolecule.org [52].

#### 4.3.2. QSAR analysis

QSAR models were generated by QSAR software of MOE 2008, the structures were built using builder tool the energy minimization was performed using MMFF94x force field. The  $pIC_{50}$  values were calculated using ( $-\log IC_{50}$ ). A large number of 2D and 3D descriptors were calculated, predicted  $pIC_{50}$  for the data set were calculated and QSAR models were validated by using the  $r^2$ , RMSE and residual values between expected and predicted  $pIC_{50}$ .

#### 4.3.3. Pharmacophore generation

The pharmacophore was built using (MOE;2008.10 software), flexible alignment protocol was applied for the best five active antiviral compounds, the molecules were adjusted and resulted in the best alignment mode. Pharmacophore query editor was used to create the pharmacophore features. The features were neither permissive nor excessively restrictive, the scheme of annotation was selected to be "Unified", the model of building was set "Consensus method", the tolerance was set 0.32 Å and the threshold was set to 99%.

#### Acknowledgments

The authors extend their deepest appreciation to Dr. Essam Rashwan, head of confirmatory diagnostic unit, Vacsera-Egypt, for helping in performing the HAV 3C<sup>pro</sup> and HRV 3C<sup>pro</sup> determination assays.

#### References

- [1] V. R. Racaniello, Picornaviridae: the viruses and their replication, in: D. M. Knipe, P. M. Howley (Eds.), Fields virology, 4th ed, Lippincott/Raven, Philadelphia, PA, 2001, pp 685–722.

- [2] L. Tong, Viral proteases, *Chem. Rev.* 102 (2002) 4609-4626.
- [3] D. Sun, S. Chen, A. Cheng, M. Wang, Roles of the Picornaviral 3C Proteinase in the Viral Life Cycle and Host Cells, *Viruses* 8 (2016) 82.
- [4] World Health Organization. Hepatitis A. <http://www.who.int/mediacentre/factsheets/fs328/en/>.
- [5] F. B. Hollinger, S. U. Emerson, Hepatitis A virus, in: D. M. Knipe, P. M. Howley, D. E. Griffin, R. A. Lamb, M. A. Martin, B. Roizman, S. E. Straus (Eds.), *Fields virology*, 5th ed, Lippincott Williams and Wilkins, Philadelphia, PA, 2007, pp 911-947.
- [6] R. S. Koff, Hepatitis A, *Lancet* 351 (1998) 1643-1649.
- [7] O. Detry, A. De Roover, P. Honore, M. Meurisse, Brain edema and intracranial hypertension in fulminant hepatic failure: pathophysiology and management, *World J. Gastroenterol.* 12 (2006) 7405-7412.
- [8] R. M. Taylor, T. Davern, S. Munoz, S. H. Han, B. McGuire, A. M. Larson, L. Hynan, W. M. Lee, R. J. Fontana, Fulminant hepatitis A virus infection in the United States: Incidence, prognosis, and outcomes, *Hepatology* 44 (2006) 1589-1597.
- [9] Z. Cao, Y. Ding, Z. Ke, L. Cao, N. Li, G. Ding, Z. Wang, W. Xiao, Luteoloside Acts as 3C Protease Inhibitor of Enterovirus 71 In Vitro, *PLoS One* 11 (2016) e0148693.
- [10] C. Yao, C. Xi, K. Hu, W. Gao, X. Cai, J. Qin, S. Lv, C. Du, Y. Wei, Inhibition of enterovirus 71 replication and viral 3C protease by quercetin, *Viol. J.* 15 (2018) 116.
- [11] Y. J. Lin, Y. C. Chang, N. W. Hsiao, J. L. Hsieh, C. Y. Wang, S. H. Kung, F. J. Tsai, Y. C. Lan, C. W. Lin, Fisetin and rutin as 3C protease inhibitors of enterovirus A71, *J. Virol. Methods.* 182 (2012) 93-98.
- [12] C. Conti, L. Proietti Monaco, N. Desideri, 3-Phenylalkyl-2H-chromenes and -chromans as novel rhinovirus infection inhibitors, *Bioorg. Med. Chem.* 25 (2017) 2074-2083.
- [13] C. Conti, L. Proietti Monaco, N. Desideri, Design, synthesis and in vitro evaluation of novel chroman-4-one, chroman, and 2H-chromene derivatives as human rhinovirus capsid-binding inhibitors, *Bioorg. Med. Chem.* 19 (2011) 7357-7364.

- [14] C. Conti, N. Desideri, New 4*H*-chromen-4-one and 2*H*-chromene derivatives as anti-picornavirus capsid-binders, *Bioorg. Med. Chem.* 18 (2010) 6480-6488.
- [15] C. Conti, N. Desideri, Synthesis and antirhinovirus activity of new 3-benzyl chromene and chroman derivatives, *Bioorg. Med. Chem.* 17 (2009) 3720-3727.
- [16] C. Conti, L. Proietti Monaco, N. Desideri, Synthesis and anti-rhinovirus activity of novel 3-[2-(pyridinyl)vinyl]substituted -2*H*-chromenes and -4*H*-chromen-4-ones, *Bioorg. Med. Chem.* 22 (2014) 1201-1207.
- [17] R. Z. Batran, A. F. Kassem, E. M. H. Abbas, S. A. Elseginy, M. M. Mounier, Design, synthesis and molecular modeling of new 4-phenylcoumarin derivatives as tubulin polymerization inhibitors targeting MCF-7 breast cancer cells, *Bioorg. Med. Chem.* 26 (2018) 3474-3490.
- [18] R. Z. Batran, D. H. Dawood, S. A. El-Seginy, T. J. Maher, K. S. Gugnani, A. N. Rondon-Ortiz, Coumarinyl pyranopyrimidines as new neuropeptide S receptor antagonists; design, synthesis, homology and molecular docking, *Bioorg. Chem.* 75 (2017) 274-290.
- [19] R. Z. Batran, D. H. Dawood, S. A. El-Seginy, M. M. Ali, T. J. Maher, K. S. Gugnani, A. N. Rondon-Ortiz, New coumarin derivatives as anti-breast and anti-cervical cancer agents targeting VEGFR-2 and p38 $\alpha$  MAPK, *Arch. Pharm. (Weinheim)* 350 (2107) e1700064.
- [20] N. A. Abdel Latif, R. Z. Batran, M. A. Khedr, M. M. Abdalla, 3-Substituted-4-hydroxycoumarin as a new scaffold with potent CDK inhibition and promising anticancer effect: Synthesis, molecular modeling and QSAR studies, *Bioorg. Chem.* 67 (2016) 116-129.
- [21] J. Neyts, E. De Clercq, R. Singha, Y. H. Chang, A. R. Das, S. K. Chakraborty, S. C. Hong, S. C. Tsay, M. H. Hsu, J. R. Hwu, Structure-activity relationship of new anti-hepatitis C virus agents: heterobicycle-coumarin conjugates, *J. Med. Chem.* 52 (2009) 1486-1490.
- [22] C. T. Chang, S. L. Doong, I. L. Tsai, I. S. Chen, Coumarins and anti-HBV constituents from *Zanthoxylum schinifolium*, *Phytochemistry* 45 (1997) 1419-1422.
- [23] N. A. Al-Masoudi, I. A. Al-Masoudi, I. A. Ali, Y. A. Al-Soud, B. Saeed, P. La Colla, Amino acid derivatives. Part I. Synthesis, antiviral and antitumor evaluation of new alpha-amino acid esters bearing coumarin side chain, *Acta Pharm.* 56 (2006) 175-188.

- [24] O. M. Abd Elhafez, Eel. D. El Khriy, F. Badria, Ael. D. Fathy, Synthesis and biological investigations of new thiazolidinone and oxadiazoline coumarin derivatives, *Arch. Pharm. Res.* 26 (2003) 686-696.
- [25] H. A. Garro, C. R. Pungitore, Coumarins as potential inhibitors of DNA polymerases and reverse transcriptases. Searching new antiretroviral and antitumoral Drugs, *Curr. Drug Discov. Technol.* 12 (2015) 66-79.
- [26] L. M. Bedoya, M. Beltrán, R. Sancho, D. A. Olmedo, S. Sánchez-Palomino, E. del Olmo, J. L. López-Pérez, E. Muñoz, A. San Feliciano, J. Alcamí, 4-Phenylcoumarins as HIV transcription inhibitors, *Bioorg. Med. Chem. Lett.* 15 (2005) 4447-4450.
- [27] N. Márquez, R. Sancho, L. M. Bedoya, J. Alcamí, J. L. López-Pérez, A. S. Feliciano, B. L. Fiebich, E. Muñoz, Mesuol, a natural occurring 4-phenylcoumarin, inhibits HIV-1 replication by targeting the NF-kappaB pathway, *Antiviral Res.* 66 (2005) 137-145.
- [28] E. M. Flefel, W. A. Tantawy, W. I. El-Sofany, M. El-Shahat, A. A. El-Sayed, D. N. Abd-Elshafy, Synthesis of some new pyridazine derivatives for anti-HAV evaluation, *Molecules* 22 (2017) pii: E148.
- [29] A. A. El-Sayed, M. El-Shahat, S. T. Rabie, E. M. Flefel, D. N. Abd-Elshafy, New pyrimidine and fused pyrimidine derivatives: Synthesis and anti hepatitis A virus (HAV) evaluation, *Int. J. Pharm.* 5 (2015) 69–79.
- [30] A. A. Abdel-Rahman, T. Wada, Synthesis and antiviral evaluation of 5-(1,2,3-triazol-1-yl methyl) uridine derivatives, *Z. Naturforsch. C* 64 (2009) 163-166.
- [31] A. H. Shamroukh, M. A. Ali, Anti-HAV activity of some newly synthesized triazolo[4,3-b]pyridazines, *Arch. Pharm. (Weinheim)* 341 (2008) 223-230.
- [32] A. E. Rashad, M. I. Hegab, R. E. Abdel-Megeid, J. A. Micky, F. M. Abdel-Megeid, Synthesis and antiviral evaluation of some new pyrazole and fused pyrazolopyrimidine derivatives, *Bioorg. Med. Chem.* 16 (2008) 7102-7106.
- [33] A. E. Rashad, M. S. Mohamed, M. E. Zaki, S. S. Fatahala, Synthesis and biological evaluation of some pyrrolo[2,3-d]pyrimidines, *Arch. Pharm. (Weinheim)* 339 (2006) 664–669.
- [34] M. T. Abdel-Aal, W. A. El-Sayed, el-S. H. El-Ashry, Synthesis and antiviral evaluation of some sugar arylglycinoylhydrazones and their oxadiazoline derivatives, *Arch. Pharm. (Weinheim)* 339 (2006) 656–663.

- [35] A. H. Halawa, A. A. Hassan, M. A. El-Nassag, M. M. Abd El-All, G. A. Abd El-Jaleel, E. M. Eliwa, A. H. Bedair, Synthesis, reactions, antioxidant and anticancer evaluation of some novel coumarin derivatives using ethyl 2-(2-oxo-4-phenyl-2H-chromen-7-yl)oxy) acetate as a starting material, *Eur. J. Chem.* 5 (2014) 111-121.
- [36] <http://www.rcsb.org>.
- [37] J. Yin, E. M. Bergmann, M. M. Cherney, M. S. Lall, R. P. Jain, J. C. Vederas, M. N. James, Dual modes of modification of hepatitis A virus 3C protease by a serine-derived beta-lactone: selective crystallization and formation of a functional catalytic triad in the active site, *J. Mol. Biol.* 354 (2005) 854-871.
- [38] J. Yin, M. M. Cherney, E. M. Bergmann, J. Zhang, C. Huitema, H. Pettersson, L. D. Eltis, J. C. Vederas, M. N. James, An episulfide cation (thiiranium ring) trapped in the active site of HAV 3C proteinase inactivated by peptide-based ketone inhibitors, *J. Mol. Biol.* 361 (2006) 673-686.
- [39] [https://www.chemcomp.com/MOE-Molecular\\_Operating\\_Environment.htm](https://www.chemcomp.com/MOE-Molecular_Operating_Environment.htm).
- [40] <http://autodock.scripps.edu/wiki/AutoDock4>.
- [41] MOE, Chemical Computing Group: Montreal, H3A 2R7 Canada, 2007.
- [42] R. Kiralj, M. M. C. Ferreira, Basic validation procedures for regression models in QSAR and QSPR studies: theory and application, *J. Braz. Chem. Soc.* 20 (2009) 770-787.
- [43] G. Cruciani, P. Crivori, P. A. Carrupt, B. Testa, Molecular fields in quantitative structure-permeation relationships: the VolSurf approach, *J. Mol. Struct. (THEOCHEM)* 503 (2000) 17-30.
- [44] C. A. Lipinski, F. Lombardo, B. W. Dominy, P. J. Feeney, Experimental and computational approaches to estimate solubility and permeability in drug discovery and development settings, *Adv. Drug Deliv. Rev.* 46 (2001) 3-26.
- [45] K. Palm, P. Stenberg, K. Luthman, P. Artursson, Polar molecular surface properties predict the intestinal absorption of drugs in humans, *Pharm. Res.* 14 (1997) 568-571.
- [46] L. L. Woods, J. Sapp, A New One-Step Synthesis of Substituted Coumarins, *J. Org. Chem.* 27 (1962) 3703-3705.

- [47] M. M. Garazd, Ya. L. Garaz, M. N. Smirnov, V. P. Khilya, Synthesis of amino acid derivatives of 7-methoxycarbonylneoflavones, *Chem. Nat. Compd.* 35 (1999) 415-419.
- [48] G. Karber, 50% end-point calculation, *Arch. Exp. Pathol. Pharmacol.* 162 (1931) 480–483.
- [49] B. S. A. Nabil, R. Zyed, A. L. Mohamed, S. Souad, A. Mahjoub, Assessment of the cytotoxic effect and in vitro evaluation of the anti-enteroviral activities of plants rich in flavonoids, *J. App. Pharm. Sci.* 2 (2012) 74-78.
- [50] C. Huitema, J. Zhang, J. Yin, M. N. James, J. C. Vederas, L. D. Eltis, Heteroaromatic ester inhibitors of hepatitis A virus 3C proteinase: Evaluation of mode of action, *Bioorg. Med. Chem.* 16 (2008) 5761-5777.
- [51] Y. Cheng, W. H. Prusoff, Relationship between the inhibition constant ( $K_i$ ) and the concentration of inhibitor which causes 50 per cent inhibition ( $I_{50}$ ) of an enzymatic reaction, *Biochem. Pharmacol.* 22 (1973) 3099-3108.
- [52] J. Jiménez, M. Škalič, G. Martínez-Rosell, G. De Fabritiis,  $K_{DEEP}$ : Protein-Ligand Absolute Binding Affinity Prediction via 3D-Convolutional Neural Networks, *J. Chem. Inf. Model.* 58(2018)287-296.

## List of tables

Table1. Cytotoxicity and antiviral effect of the synthesized compounds

Compounds µg/ml	CC <sub>50</sub>	Virucidal effect		Effect on viral adsorption		Effect on viral replication	
		IC <sub>50</sub>	TI	IC <sub>50</sub>	TI	IC <sub>50</sub>	TI
<b>1</b>	340	4.8	70.8	1133.3	0.3	42.5	8
<b>2</b>	900	1285.7	0.7	180	5	25.7	35
<b>3</b>	785	3925	0.2	112	7	1121.4	0.7
<b>4</b>	367	4.7	78	183.5	2	7.34	50
<b>5a</b>	897	44.8	20	112	8	35.8	25
<b>5b</b>	245	81.6	3	3.18	77	0.75	32
<b>5c</b>	249	9.9	25	9.9	25	622.5	0.4
<b>6</b>	648	216	3	3240	0.2	72	9
<b>7a</b>	951	237.7	4	11.88	80	63.4	15
<b>7b</b>	258	3.1	83	32.25	8	86	3
<b>8a</b>	435	2175	0.2	543.7	0.8	145	3
<b>8b</b>	129	64.5	2	18.4	7	25.8	5
<b>9a</b>	648	11.3	57	1296	0.5	13.5	48
<b>9b</b>	597	12.9	46	49.7	12	82.7	7
<b>10</b>	942	47	20	1177.5	0.8	13.4	70
<b>11</b>	753	37.6	20	83.6	9	44.3	17
<b>12</b>	951	105.6	9	13	72	1358.5	0.7
<b>13a</b>	483	80.5	6	241.5	2	120.7	4
<b>13b</b>	549	784.3	0.7	1098	0.5	5490	0.1
<b>13c</b>	951	13	73	21.6	44	18.3	52
<b>14a</b>	438	109.5	4	219	2	730	0.6
<b>14b</b>	978	30.5	32	44.4	22	10.7	91
<b>14c</b>	752	1880	0.4	8.5	88	62.6	12
<b>Acyclovir</b>	> 1000	35.6	80	33.5	85	30.6	93

**Table 2. Inhibition effect of compounds 7b, 14b and 14c against HAV 3C and HRV 3C proteases**

Compound	IC <sub>50</sub> (μM) HAV 3C protease	Ki (μM) HAV 3C protease	IC <sub>50</sub> (μM) HRV 3C protease
7b	17.78	1.903	16.10
14b	5.94	0.104	4.13
14c	7.19	0.217	6.30

**Table 3. Interactions between the atoms/groups of the compounds and the residues**

Compounds	atom/group contribute in H-bond formation	Residues	Distance Å
<b>Tetrapeptidyl inhibitor</b>	P1-Glutamine	Cys172	Covalent bond
		NH-Cys172	2.8
	P3-phenylalanine	NH-Gly170	2.8
		OH-Val144	3.0
	P4-leucin.	OH-Gly194	2.9
		NH-Val144	3.0
<b>7b</b>	O atom of C=O	OH-Gly194	3.0
		SH-Cys172	3.2
		SH-Cys172	2.8
		NH-Cys172	3.1
	O atom of C-O	NH-Gly170	2.7
		NH-His44	3.3
	S of C=S	NH-His191	3.1
O atom of C=O	Nh-Gly194	2.9	
<b>14b</b>	O atom of C=O	SH-Cys172	3.1
		SH-Cys172	2.5
		NH-Cys172	3.1
		NH-Gly170	2.7
<b>14c</b>	O atom of C=O	SH-Cys172	2.9
		SH-Cys172	3.1
		NH-Cys172	2.9
		NH-Gly170	2.8

**Table 4. Binding free energy and binding affinity of compounds 7b, 14b and 14c**

Comp.	Binding free energy ( $\Delta G_{\text{Bind}}$ )	Binding affinity ( $\text{pK}_d$ )
	kcal/mol	
7b	-9.15	6.78
14b	-7.44	5.51
14c	-7.47	5.53

**Table 5. Experimental and predicted antiviral activity of the synthesized compounds by QSAR model.**

Comp. No.	Experimental $\text{PIC}_{50}$	Predicted $\text{PIC}_{50}$	Residual	Z-score
1	4.69	4.64	0.04	0.24
4	4.87	5.05	-0.18	0.93
5a	3.97	3.89	0.07	0.39
5b	3.74	3.86	-0.12	0.64
5c	4.67	4.71	-0.04	0.24
7a	3.20	3.36	-0.16	0.83
7b	5.10	4.96	0.13	0.68
8b	3.70	3.38	0.31	1.59
9a	4.50	4.47	0.04	0.21
9b	3.37	3.41	-0.04	0.22
10	4.02	3.81	0.20	1.00
11	3.99	3.95	0.03	0.17
12	3.62	3.44	0.17	0.88
13a	3.73	3.62	0.10	0.52
13b	2.78	3.13	-0.35	1.75
13c	4.60	4.55	0.04	0.28
14a	3.50	4.06	-0.49	2.47
14b	4.16	3.92	0.23	1.17

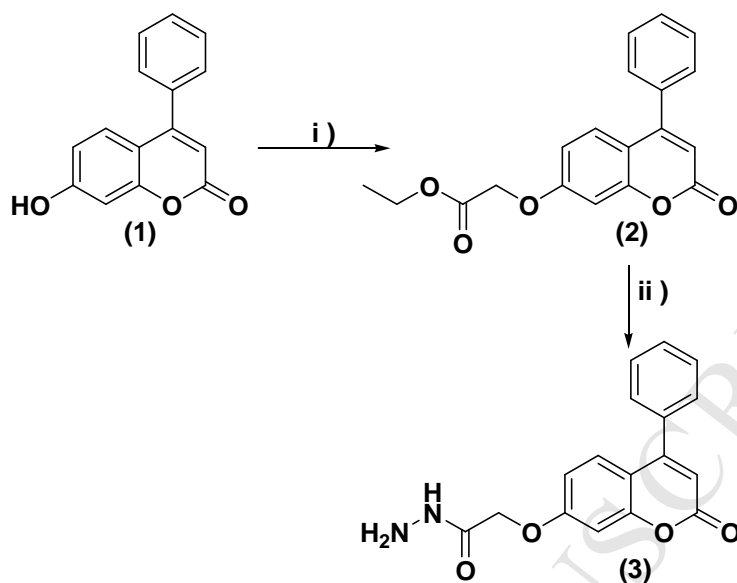
**Table 6. Constraint distance and angles between features of the generated top pharmacophore model**

Features	Constratint distance (Å)	Features	Angles (°)
F1-F5	6.07	F1-F6-F5	34.1
F1-F2	2.65	F1-F2-F5	148.9
F2-F4	3.38	F1-F2-F5	95.5
F5-F4	5.26	F1-F3-F7	122.5
F1-F7	7.17		
F3-F7	5.21		
F1-F6	9.60		
F5-F6	10.77		

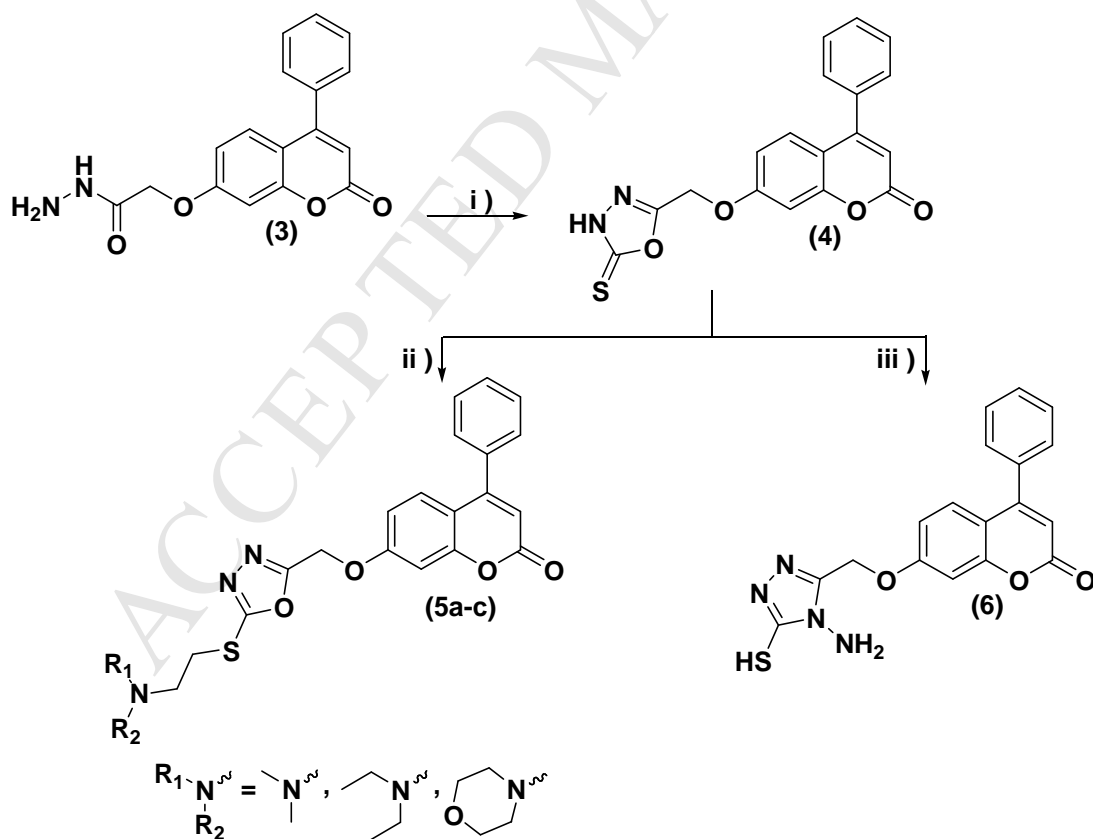
Table 7. Calculated Lipinski's rule criteria of the synthesized compounds

Comp.No.	M.Wt	No. of HBD	No. of HBA	Log p	Log S	PSA(Å <sup>2</sup> )
1	238.24	1	2	3.6	-4.1	46.5
2	324.33	0	3	3.7	-5.3	61.8
3	310.30	2	4	2.2	-4.8	90.6
4	352.36	0	4	4.4	-7.0	113.2
5a	423.48	0	5	4.4	-7.0	77.6
5b	451.54	0	5	5.1	-7.6	77.6
5c	465.52	0	6	3.9	-7.2	86.9
6	366.93	1	4	3.00	-6.3	131.0
7a	383.42	3	4	2.7	-5.9	120.7
7b	397.45	3	4	3.0	-6.2	120.7
8a	365.41	1	4	4.4	-5.9	70.43
8b	379.43	1	4	4.7	-6.2	73.34
9a	365.41	0	4	5.5	-6.5	103.4
9b	379.43	0	4	5.8	-6.8	103.4
10	492.59	0	6	4.5	-6.8	78.7
11	374.39	0	4	4.1	-5.7	70.42
12	440.40	1	5	4.1	-7.2	102.0
13a	439.42	2	5	4.1	-7.4	106.0
13b	473.86	2	5	4.7	-8.1	106.0
13c	518.32	2	5	4.9	-8.5	106.0
14a	412.44	1	4	5.4	-7.0	76.9
14b	446.88	1	4	6.0	-7.8	76.9
14c	491.33	1	4	6.2	-8.1	76.9

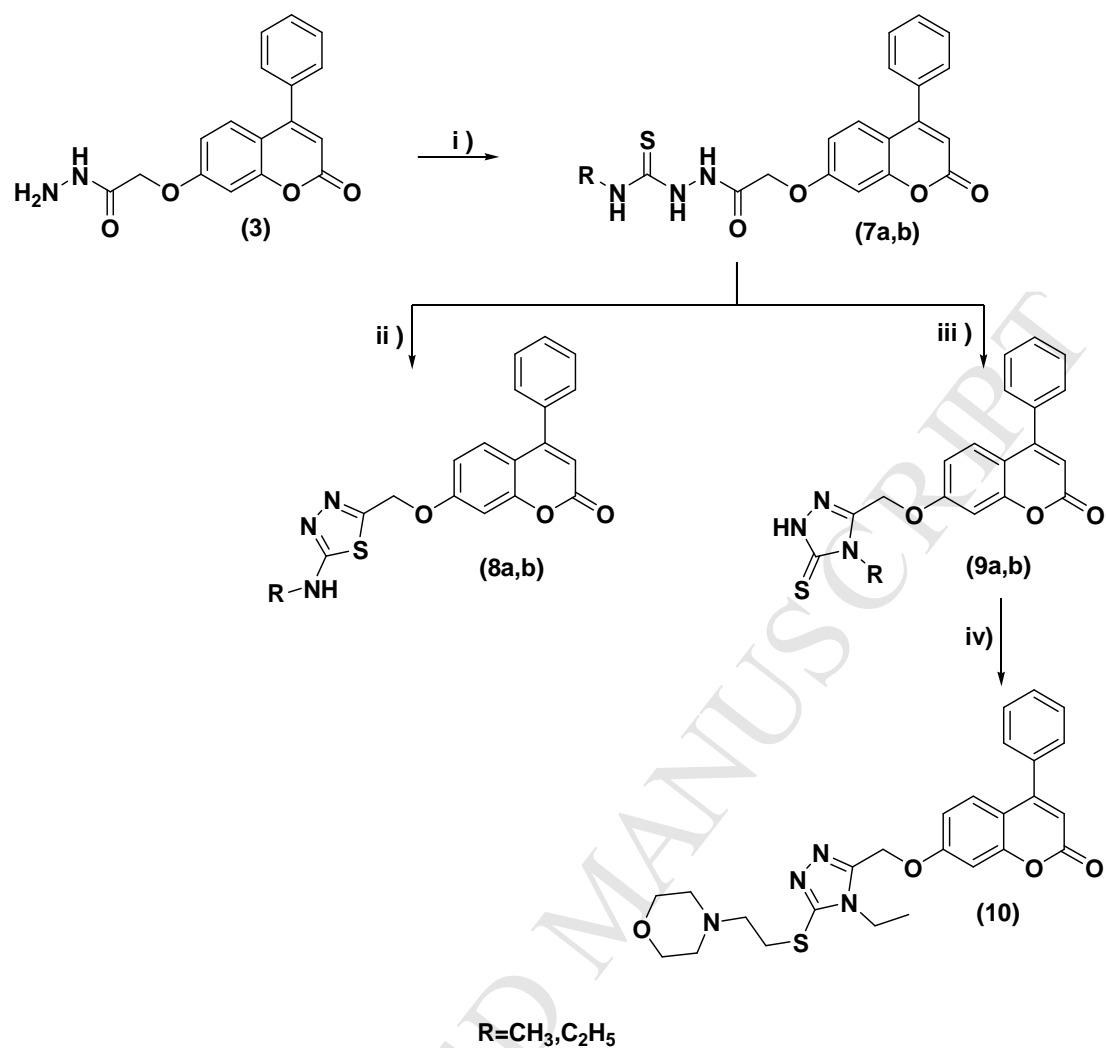
## List of schemes



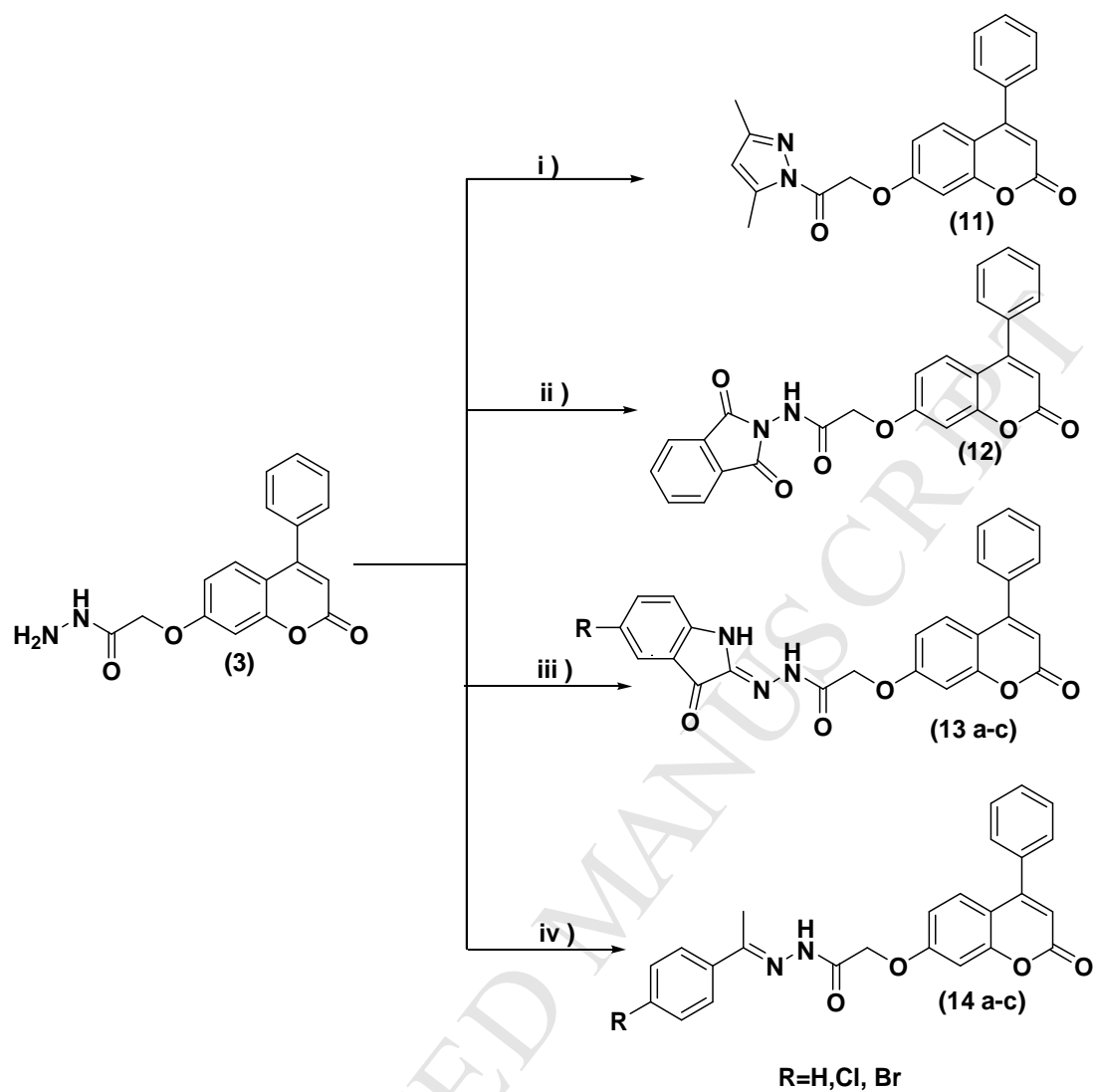
**Scheme 1.** i)  $\text{C}_2\text{H}_5\text{OCOCH}_2\text{Br}$ , anhydrous  $\text{K}_2\text{CO}_3$ , acetone, reflux, ii)  $\text{NH}_2\text{NH}_2 \cdot \text{H}_2\text{O}$ , EtOH, RT



**Scheme 2.**i)  $\text{CS}_2$ , pyridine, reflux, ii)  $\text{N}(\text{R}_1)(\text{R}_2)\text{CH}_2\text{CH}_2\text{Cl} \cdot \text{HCl}$ , anhydrous  $\text{K}_2\text{CO}_3$ , acetone, reflux, iii)  $\text{NH}_2\text{NH}_2 \cdot \text{H}_2\text{O}$ , EtOH, reflux.



**Scheme 3.** i) RNCS, EtOH, reflux, ii) H<sub>2</sub>SO<sub>4</sub>, RT, iii) 2N KOH, reflux, iv) 2-Morpholinoethyl chloride hydrochloride, anhydrous K<sub>2</sub>CO<sub>3</sub>, acetone, reflux.



**Scheme 4.** **i)**  $\text{CH}_2(\text{COCH}_3)_2$ , EtOH, reflux, **ii)** phthalic anhydride, AcOH, reflux, **iii)** isatin derivatives, AcOH, reflux, **iv)**  $\text{ArCOCH}_3$ , EtOH, AcOH, reflux.

## List of Figures

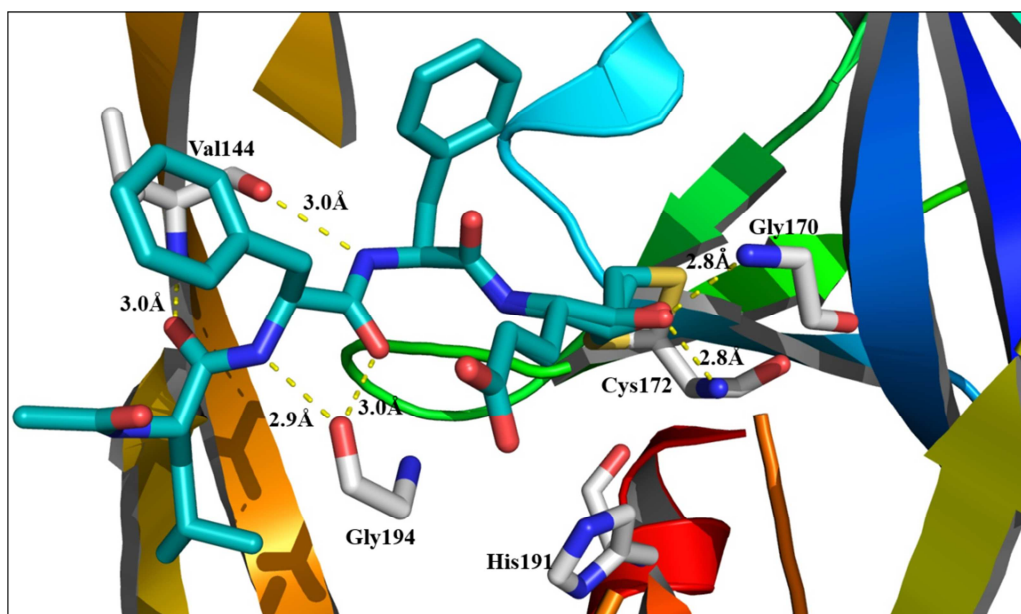


**Fig.1.** Tetrapeptidyl inhibitor (cyan stick) formed two covalent bonds between P1-Glutamine and Cys172 in addition to one H-bond with Gly170. P3-phenylalanine formed two H-bonds with Val144 and Gly194, and P4-Leucin contributed by two H-bonds with Val144 and Gly194.

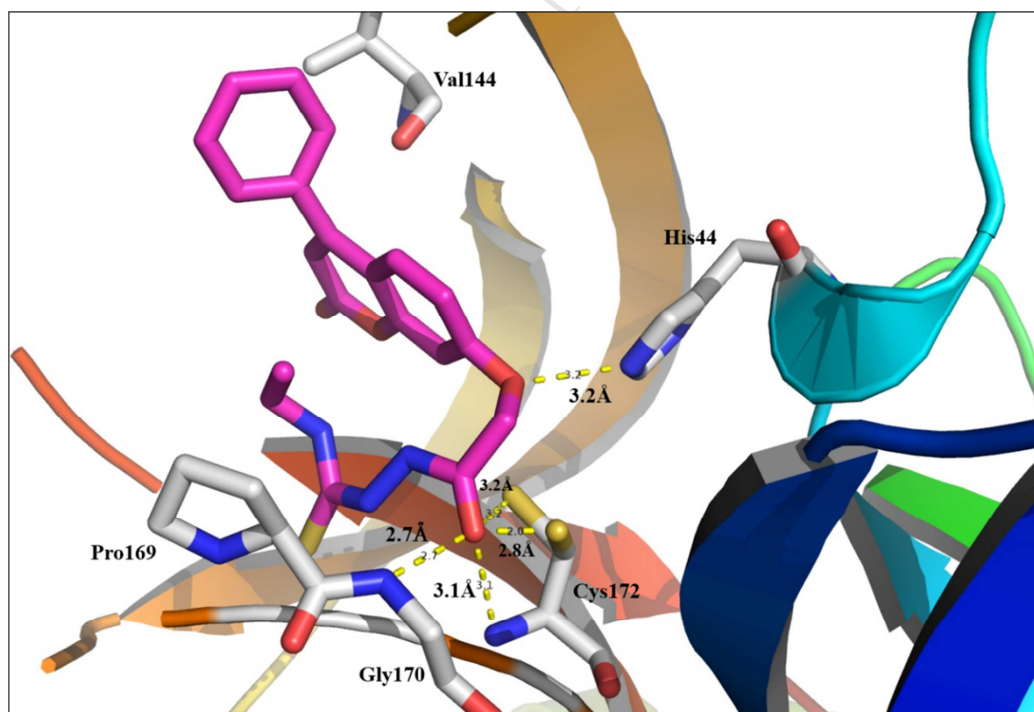


**Fig.2A.** Interactions of compound **7b** (pink stick), it formed five H-bonds with His44, Gly170 and Cys172 (grey, stick), protein represented as cartoon.

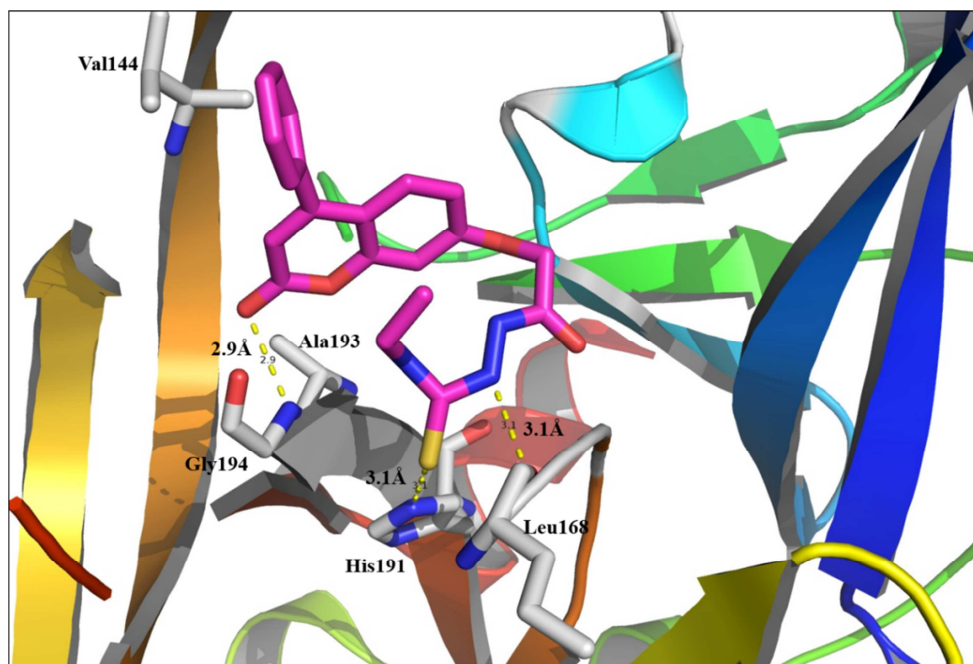


**Fig.2B.** Another view of interactions of compound **7b** (pink stick) with Leu168, His191 and Gly194 (grey stick).

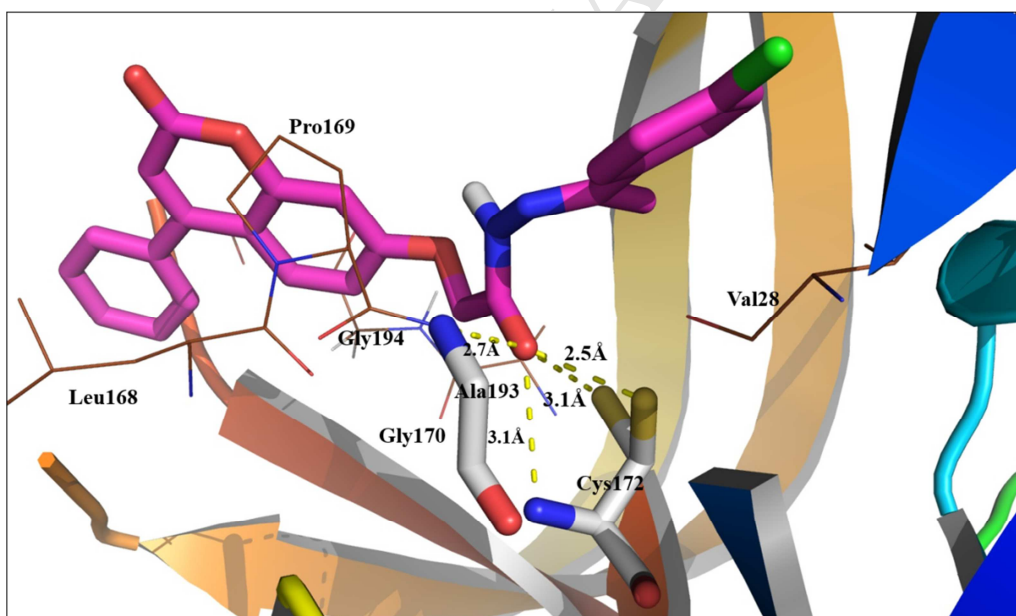


**Fig.3.** Interactions of compound **14b** (pink stick), it formed four H-bonds with Gly170 and Cys172 (grey stick), 4-phenycoumarin moiety showed hydrophobic interactions with Leu168, pro169, Ala193 and hydrophobic part of Gly194 and Gly195 (brown line).

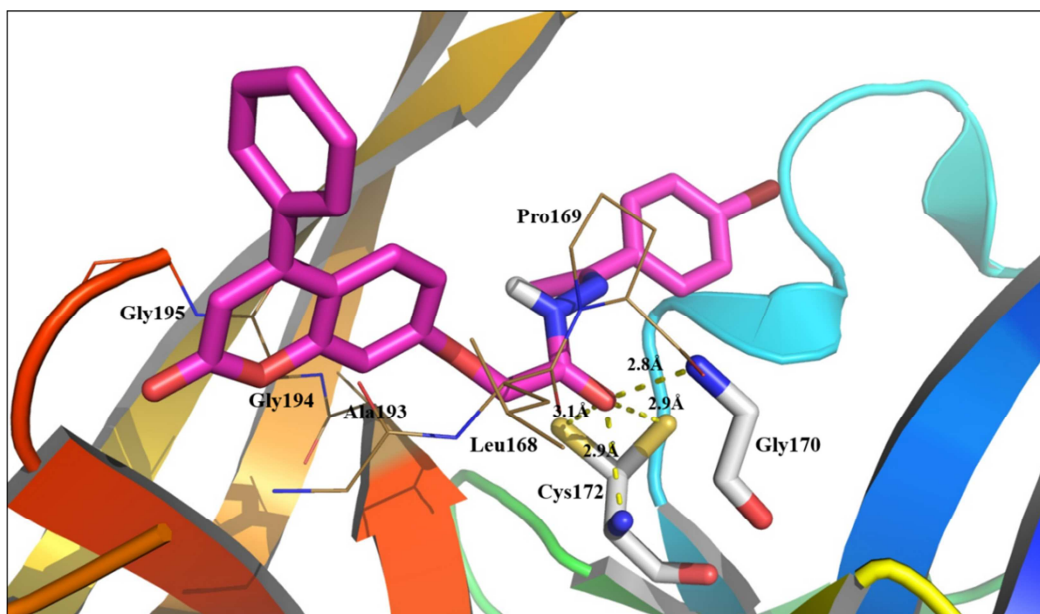


**Fig.4.** Interactions of compound **14c** (pink stick), it formed four H-bonds with Gly170 and Cys172 (grey stick), 4-phenylcoumarin moiety showed hydrophobic interactions with Leu168, pro169, Ala193 and hydrophobic part of Gly194 and Gly195 (brown line).

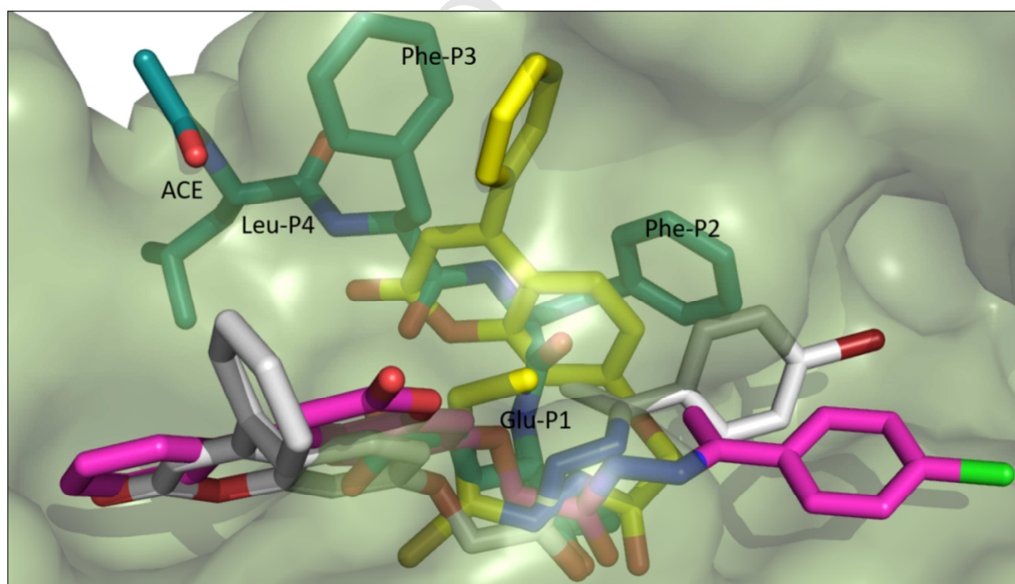


**Fig.5.** Binding mode of tetrapeptidyl inhibitor (dark cyan), compound **7b** (yellow stick), compound **14b** (pink stick) and **14c** (white stick).

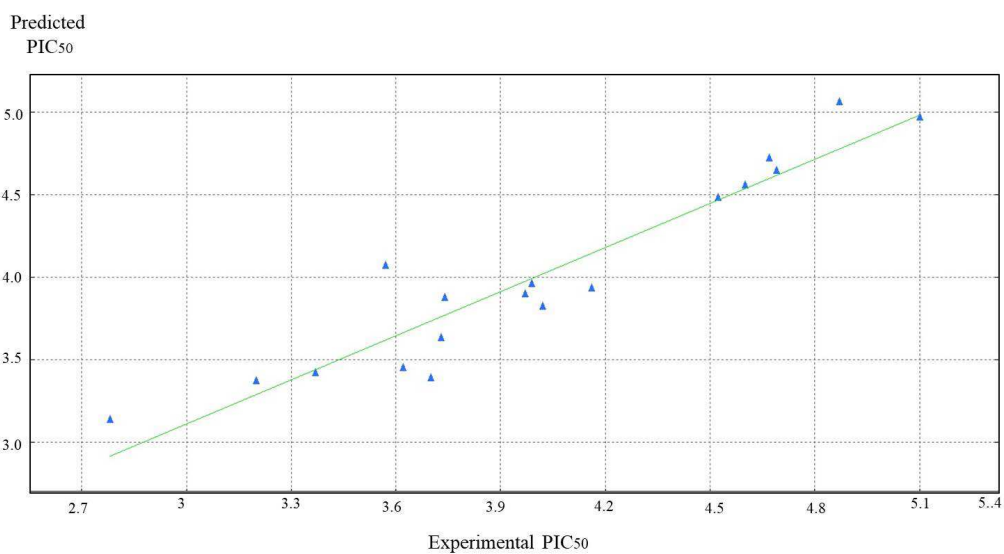


**Fig.6.** Correlation plot of experimental  $pIC_{50}$  versus predicted  $pIC_{50}$ .

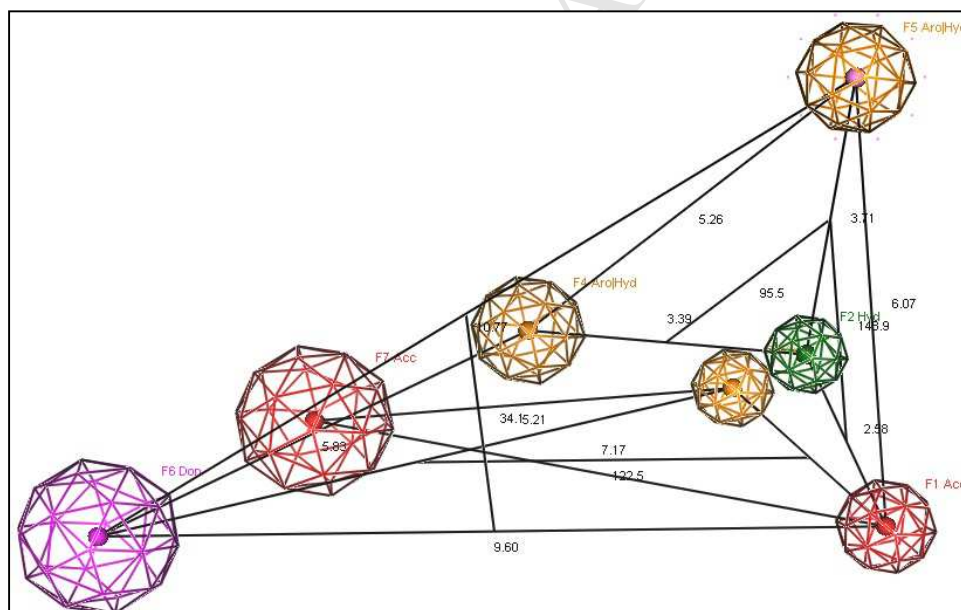
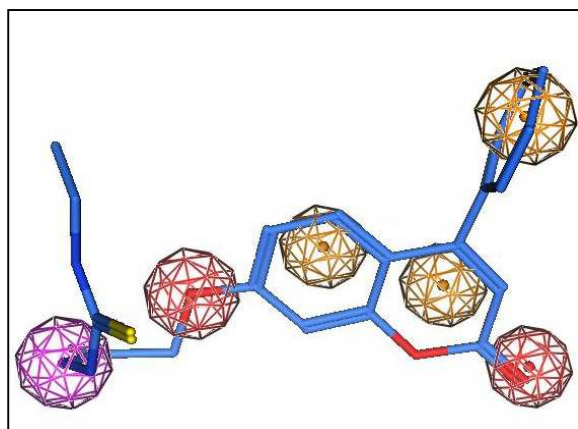


**Fig.7.** Constraint distances and angles between features of the generated top pharmacophore model. Features; hydrogen bond acceptor (HBA) red, hydrogen bond donor (HBA) pink, hydrophobic (HYD) green and ring aromatic (RA) orange.

A



B

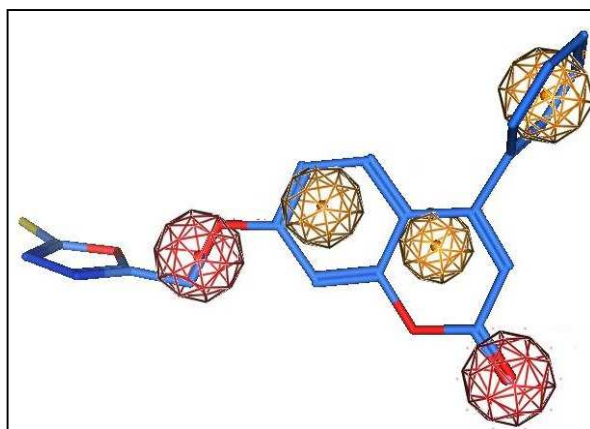


**Fig.8.** A) Compound **7b** fitted within the pharmacophore model, B) compound **4** fitted within the pharmacophore model.

### Highlights

- A new series of 4-phenylcoumarin derivatives was designed and synthesized.
- Compound **7b** was the most potent virucidal agent.
- **14b** and **14c** showed virustatic effects against viral replication and adsorption.
- **7b**, **14b** and **14c** showed potent inhibition effect against HAV3C<sup>pro</sup> and HRV3C<sup>pro</sup>.
- Molecular docking, QSAR and 3D-pharmacophore analyses were performed.